

Sodium Periodate Mediated Oxidative Extraction of Polysaccharide-derived Structures from Wood Biomass: Influence of Reaction Time and Oxidation

Downloaded from: https://research.chalmers.se, 2026-11-13 18:11 UTC

Citation for the original published paper (version of record):
Kurth de Azambuja, L., Hasani, M. (2026). Sodium Periodate Mediated Oxidative Extraction of Polysaccharide-derived Structures from Wood
Biomass: Influence of Reaction Time and Oxidation Conditions in Birch and Spruce. BioResources, 21(2): 2960-2979. http://dx.doi.org/10.15376/biores.21.2.2960-2979

N.B. When citing this work, cite the original published paper.

research.chalmers.se offers the possibility of retrieving research publications produced at Chalmers University of Technology. It covers all kind of research output: articles, dissertations, conference papers, reports etc. since 2004. research.chalmers.se is administrated and maintained by Chalmers Library

(article starts on next page)

THESIS FOR THE DEGREE OF LICENTIATE OF ENGINEERING

Oxidative recovery of hemicelluloses from lignocellulosic biomass

Influence of periodate oxidation conditions and cell wall accessibility

LUCAS KURTH DE AZAMBUJA

Department of Chemistry and Chemical Engineering

CHALMERS UNIVERSITY OF TECHNOLOGY

Gothenburg, Sweden 2026

Oxidative recovery of hemicelluloses from lignocellulosic biomass
Influence of periodate oxidation conditions and cell wall accessibility

LUCAS KURTH DE AZAMBUJA

© LUCAS KURTH DE AZAMBUJA, 2026.

Nr. 2026:06

Department of Chemistry and Chemical Engineering
Chalmers University of Technology
SE-412 96 Gothenburg
Sweden
Telephone + 46 (0)31-772 1000

Cover: Illustration by Lucas Kurth de Azambuja

Printed by Chalmers Digitaltryck
Gothenburg, Sweden 2026

Oxidative recovery of hemicelluloses from lignocellulosic biomass

LUCAS KURTH DEAZAMBUJA

Department of Chemistry and Chemical Engineering
Chalmers University of Technology

ABSTRACT

Lignocellulosic biomass is one of the most abundant renewable resources for the production of materials, chemicals, and fuels. Among its components, hemicelluloses are versatile polysaccharides, yet methods for their selective extraction remain limited, restricting their utilization. Developing efficient strategies for hemicellulose recovery is therefore important to improve resource efficiency and enable new biorefinery pathways.

This work investigates sodium periodate oxidation as a strategy to facilitate the extraction and structural modification of hemicellulose-derived structures from wood biomass, with emphasis on oxidation conditions and cell wall accessibility.

In the first study, the effects of oxidation time and oxidant dosage were examined in hardwood (birch) and softwood (spruce). Periodate oxidation introduced aldehyde functionalities, increased extraction yields, and promoted depolymerization. Differences between hardwood and softwood extracts reflected variations in hemicellulose structure and the availability of vicinal diols.

The second study evaluated the role of cell wall accessibility using genetically modified aspen containing a callose spacer between cellulose macrofibrils and wood pretreated by peracetic acid delignification. Delignification did not substantially increase the overall extraction but enhanced the recovery of xylan-rich fractions, highlighting the limiting effect of lignin, while the callose spacer had little influence on extraction efficiency. Periodate oxidation consistently produced depolymerized oligosaccharides with a relatively narrow molar mass distribution.

Overall, the results show that sodium periodate oxidation can be used to extract and modify hemicellulose-derived structures, providing insight into how reaction conditions and biomass structure influence the process and contributing to improved fractionation strategies for lignocellulosic biorefineries.

Keywords: Hemicellulose extraction, oxidation, sodium periodate, cell wall accessibility, delignification.

LIST OF PUBLICATIONS

This thesis is based on the following appended papers:

Paper I **Sodium periodate mediated oxidative extraction of Polysaccharide-derived structures from wood biomass: influence of reaction time and oxidation conditions in birch and spruce**

BioResources 2026, *21* (2), 2960–2979. Doi: 10.15376/biores.21.2.2960-2979

Lucas Kurth de Azambuja and Merima Hasani.

Manuscript II **Unlocking hemicelluloses: the impact of lignin and cell wall architecture on oxidative extraction**

Lucas Kurth de Azambuja, Matthieu Bourdon, Ykä Helariutta and Merima Hasani.

In internal revision

CONTRIBUTION REPORT

Paper I Lucas Kurth de Azambuja (first author): methodology, experimental work, writing – original draft. Merima Hasani: conceptualization, writing – review & editing

Manuscript II Lucas Kurth de Azambuja (first author); methodology, experimental work, writing – original draft. Merima Hasani: conceptualization, writing – review & editing

Matthieu Bourdon and Ykä Helariutta: developing, growing, and providing the genetically modified raw material.

Contents

1. Introduction 1
1.1. Biorefinery and sustainability 1
1.2. Objectives 1
2. Background 3
2.1. Tree structures 3
2.1.1. Cellulose 3
2.1.2. Hemicelluloses 4
a) Hardwood hemicelluloses 5
b) Softwood hemicelluloses 6
2.1.3. Lignin 7
2.2. Hemicellulose interaction in the cell wall 7
2.3. Applications 8
2.4. Hemicellulose extraction 9
2.5. Oxidation used for biomass valorization 10
2.6. Periodate use for extraction 12
2.7. Modifications of the cell wall accessibility 14
2.7.1. Callose introduction 14
2.7.2. Peracetic acid and delignification 14
3. Materials and methods 16
3.1. Materials 16
3.2. Delignification 17
3.3. Sodium periodate oxidation 17
3.3.1. Oxidation as a function of time 17
3.3.2. Oxidation as a function of oxidant charge 17
3.3.3. $NAIO_4$ oxidation through flow reactor 18
3.4. Determination of aldehyde content 18
3.5. Measurement of periodate consumption 19
3.6. Carboxylic acid determination 19
3.7. Yield 19

3.8. Fourier transformation infrared spectroscopy analysis 20
3.9. Compositional analysis of obtained liquors and the solid residues 20
3.9.2 Carbonyl content in the pulp 21
3.10. Gel permeation chromatography 21
3.11. Nuclear magnetic resonance spectroscopy 22
4. Results and discussion 23
4.1. Oxidation effects on birch wood as a function of time 23
4.2. The impact of periodate concentration and type of biomass on the effects of oxidation/extraction 28
4.3. Impact of cell wall accessibility on the oxidative extraction 33
5. Conclusions 44
6. Acknowledgments 46
7. References 47

1. Introduction

1.1. Biorefinery and sustainability

Biorefineries are central to the transition toward a bio-based economy, aligning with global sustainability efforts by reducing reliance on fossil resources and developing renewable alternatives [1], [2], [3]. This concept is considered a practical approach to largely replace the existing fossil-based material and energy systems through the utilization of lignocellulosic biomass. [4]. They are, namely, envisioned to convert biomass into a diverse array of useful products, including biochemicals, materials, and biofuels, through environmentally benign processes [4]. This promotes efficient resource use and lower greenhouse gas emissions, thus fitting sustainable economy principles [2], [4], [5].

In this context, lignocellulosic biomass, composed of cellulose, hemicelluloses, and lignin, is a sustainable feedstock for biorefineries [4], [6]. However, challenges in deconstructing lignocellulose and converting individual components into functional bio-structures for materials and chemicals persist due to its inherent recalcitrant nature and structural complexity [7], [8]. Yet, despite the technical challenges in processing the lignocellulosic biomass, lignocellulosic biorefineries have high potential to become major providers of bio-building blocks due to the abundant availability of feedstocks along with the basic infrastructure (e.g., forest industry) for biomass processing [9].

1.2. Objectives

The main objective of this work is to address the question: can the oxidation-induced structural changes in hemicelluloses be employed to promote their extraction and recovery from lignocellulosic biomass?

The work is based on the hypothesis that conformational changes of hemicelluloses upon oxidation are capable of improving their solubility and mobility in the cell wall, leading, thus, to enhanced extractability.

To reach this objective, the following sub-objectives are addressed:

- To evaluate whether the well-studied periodate oxidation, acting through a well-known pyranose ring opening, can effectively provide hemicellulose extraction and recovery.
- To determine how oxidation parameters, such as oxidant dosage and reaction time, influence the extraction yield and the molecular characteristics of the recovered material.

- To investigate how biomass structure and cell wall accessibility influence the oxidation-mediated extraction of hemicelluloses.

2. Background

2.1. Tree structures

The main part of the globally available lignocellulosic biomass is located in trees. Trees are complex, hierarchical biological materials whose structure spans multiple length scales, from the supramolecular arrangement of polymers in the cell walls to the macroscopic organization of fibers in the trunk (Figure 1). This multiscale architecture is responsible for wood's remarkable combination of strength, stiffness, flexibility, and porosity [10], [11]. At the macroscopic level, wood is a porous material composed primarily of elongated cells aligned along the longitudinal axis of the tree. In softwoods, these are primarily tracheids (elongated cells providing both supportive and conductive function) combined with a minor content of parenchyma cells (specialized for storage and protection), while hardwoods contain a more diverse mix of fibers (support), vessels (conduction), and parenchyma cells (storage and metabolic functions) [10], [11]. Those plant cells, connected by membrane openings in their cell walls (pits), form a continuous network of interconnected cavities, or lumina, that give wood its intrinsic porosity and enable the transport of water and nutrients during the tree's life while influencing later processes like chemical modification and drying [10], [11].
The cell wall itself is a multilayered structure composed of highly organized biopolymers. At the molecular level, these layers are constructed from cellulose, hemicelluloses, and lignin [12], [13], their structural details and assembly in the cell wall layers being described below.

2.1.1. Cellulose

Cellulose forms the primary structural scaffold of the cell wall through long, linear chains of β-(1→4)-linked glucose units that assemble into tightly packed, semi-crystalline microfibrils [13]. These microfibrils aggregate into larger bundles known as macrofibrils [14], assembled in different layers of the cell wall. The outermost part of the cell wall, the primary cell wall, forms during cell growth and consists mainly of cellulose, hemicelluloses, and pectins, with cellulose microfibrils arranged in a relatively disordered network that allows for wall extensibility. When the cell growth has been completed, the secondary cell wall is deposited between the primary wall and the membrane, in three layers: S1, S2, and S3. In the thin S1 layer (0-2-03 μm), cellulose microfibrils are oriented at a relatively large angle in relation to the cell axis. The S2 layer is the thickest (1-5 μm) and contains microfibrils aligned at a significantly smaller angle to the cell axis, providing most of the mechanical

strength. In the thin S3 layer (~0.1 µm), microfibrils are again arranged at a large angle relative to the axis, forming the innermost layer adjacent to the membrane. The composition of cellulose, hemicelluloses, and lignin varies between the layers. The adjacent cells are connected by a lignin and pectin-rich layer responsible for cell adhesion, the middle lamella [15].

2.1.2. Hemicelluloses

Hemicelluloses are closely associated with the cellulose backbone of the cell wall and comprise two main groups of heteropolysaccharides: xylans and glucomannans [14]. They typically account for approximately 20–35% of the total weight of the lignocellulosic biomass, though this percentage varies significantly depending on the specific botanical species and tissue type [13], [14], [16]. Unlike cellulose, which is characterized by its linear, highly crystalline arrangement of glucose chains, hemicelluloses possess a branched and amorphous structure [2], [16], [17].

Due to their amorphous nature and lower degree of polymerization compared to cellulose, hemicelluloses are significantly more susceptible to hydrolysis, which makes them a primary target for efficient deconstruction in biorefinery processes [13], [14]. Their abundance and renewable nature, combined with their rich functional chemistry, allow for the conversion of hemicelluloses into a wide array of value-added products, including platform chemicals and advanced biomaterials [2], [13], [14].

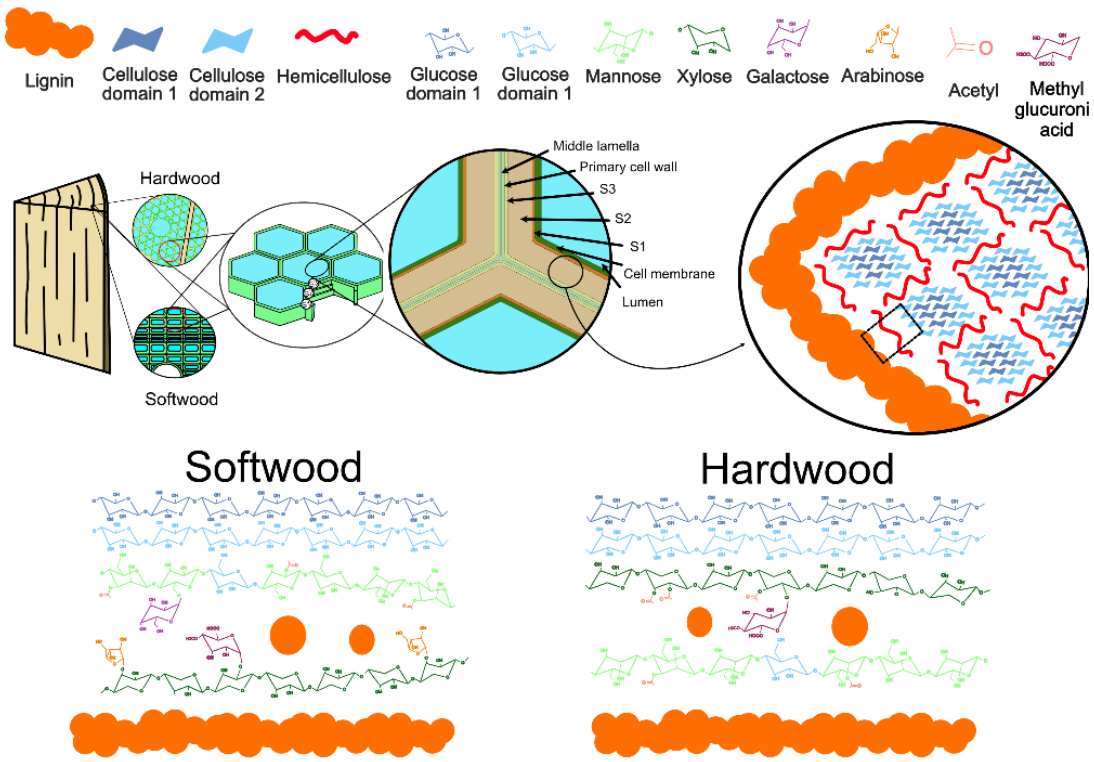


Figure 1: Schematic representation of the wood structure: cell wall, and molecular level organisation previous work [17].

a) Hardwood hemicelluloses

The dominating hemicelluloses in hardwood species are O-acetyl-4-O-methylglucuronoxylans, which consist of β-(1→4)-linked xylan backbone, (Figure 2) [17], [18] typically featuring approximately one β-(1→2)-4O-methylglucuronic acid substituent for every 10–20 xylose residues and a high degree of acetylation corresponding to approximately 0.3–0.6 mol of acetate groups per mol of xylose [16], [18].
In addition to glucuronoxylans (but in much lower amounts, typically 2-5%), hardwoods contain glucomannans, primarily O-acetylated glucomannans composed of a β-(1→4) linked backbone of mannose and glucose units [16]. Although glucuronoxylan is the dominant hemicellulose in both birch and aspen (treated in this work), compositional differences have been reported [14], [18]. Birch generally contains a slightly higher hemicellulose content, and variations also occur in the frequency and distribution of 4-O-methylglucuronic acid substituents and acetyl groups along the backbone [14].

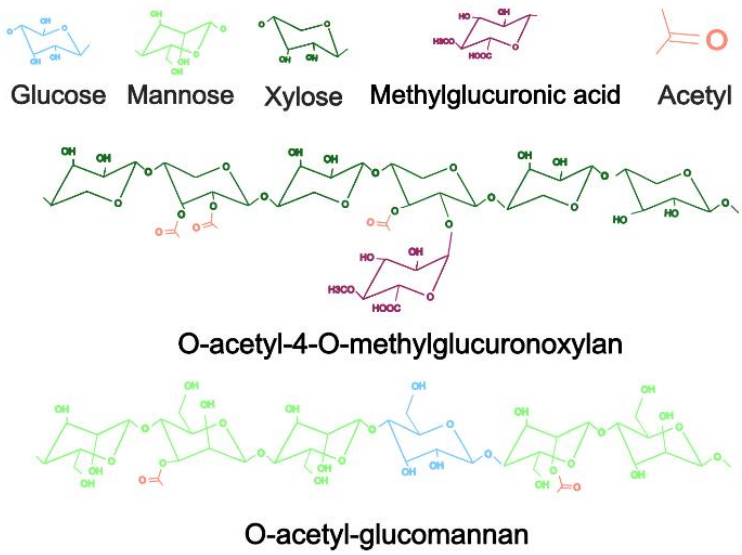


Figure 2: Hardwood hemicellulose (illustration based on the work of [17].)

b) Softwood hemicelluloses

Softwood total hemicellulose content generally ranges from approximately 25 to 30% of the dry wood weight and comprises primarily glucomannans (10–15%), along with galactoglucomannans (5–8%) and arabinoglucuronoxylans. Glucomannans consist of a β-(1→4)-linked backbone of mannose and glucose units, with the mannose-to-glucose ratio typically ranging from 3:1 to 4:1, although this can vary depending on species and growth conditions [19], [20]. Glucomannans are partially acetylated, predominantly at the C-2 and/or C-3 positions of mannose units, but their degree of acetylation is generally lower than that observed for hardwood xylans [19], [20]. Galactoglucomannans also carry α-(1→6) linked galactose substituents attached to mannose residues [16], [20] (Figure 3). In addition to galactoglucomannans, softwoods contain arabinoglucuronoxylans [17], [20], [21]. These xylans are composed of a β-(1→4)-linked xylan backbone substituted with α-(1→2)-linked 4-O-methylglucuronic acid residues and α-(1→3)-linked arabinofuranose units [22].

Overall, the predominance of glucomannans, the presence of the galactose side groups, and the specific substitution patterns of arabinoglucuronoxylans distinguish softwood hemicellulose chemistry from that of hardwoods, with important implications for pulping, fractionation strategies, and biorefinery processing routes [14].

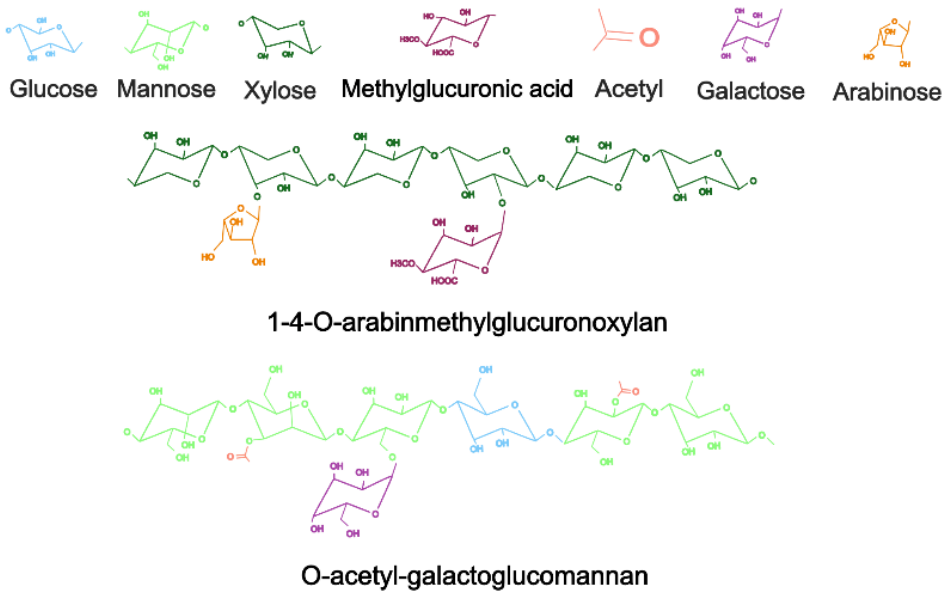


Figure 3: Schematic illustration of softwood hemicellulose (Illustration based on the work of [17])

2.1.3. Lignin

Lignin is an aromatic, three-dimensional polymer composed of phenylpropane units [23]. It acts as a natural adhesive that provides compressive strength, hydrophobicity, and resistance to decay [23], [24]. Hemicelluloses are believed to be associated with lignin through covalent bonds and physical entanglement, helping to integrate the carbohydrate network with the hydrophobic lignin matrix via the formation of lignin-carbohydrate complexes [16], [24], [25]. These dual interactions enable the distribution of mechanical stress, enhance moisture regulation, and define the architecture of the secondary cell wall [12], [16], [24].

2.2. Hemicellulose interaction in the cell wall

The structural integrity of the tree cell wall arises not only from the intrinsic properties of cellulose, hemicelluloses, and lignin but also from their intimate molecular interactions and supramolecular organization [17]. Together, they give rise to a resilient composite system in which cellulose provides strength, hemicelluloses contribute with flexibility and connectivity, and lignin ensures rigidity and protection, enabling trees to thrive in diverse and demanding environments [2], [13], [23]. Hemicelluloses exhibit distinct interaction patterns with cellulose microfibrils and lignin [17]. In general, glucomannans are believed to associate closely with cellulose surfaces through hydrogen

bonding and van der Waals forces, while xylans are believed to be more frequently linked to lignin via lignin–carbohydrate complexes [25]. These structural features influence their extractability, hydrothermal stability, and depolymerization behavior. Yet, there is a portion of xylan believed to closely interact with cellulose. When xylan interacts with the cellulose surface, its backbone geometry typically undergoes a conformational change from a flexible three-fold helical screw to a flat, two-fold helical screw ribbon [16], [26]. This conformation aligns with the periodicity of the cellulose microfibrils, maximizing interpolymer hydrogen bond formation [16], [26]. These hydrogen bonds act as reversible but numerous intermolecular interactions that restrict relative movement between adjacent microfibrils, thereby resisting shear stress and limiting fibril slippage under mechanical load [17], [26]. In addition to these directional interactions, Van der Waals forces contribute significantly to the overall attachment by promoting close surface contact and cohesive attraction between polymer chains [27].

2.3. Applications

Although hemicelluloses exhibit considerable potential, they are prone to degradation in traditional pulping operations, which hampers their practical exploitation and calls for advanced pre-extraction and modification methods to enhance their utilization in a biorefinery concept.[16]. Despite representing nearly 30% of plant biomass, they are frequently considered a waste material in a typical Kraft pulping process [28] where they are degraded into low-molecular-weight fragments, which dissolve into the black liquor alongside lignin and are subsequently burned as a low-value fuel for energy recovery [16], [29]. Yet, the attractive poly-, oligo-, and monosaccharide structures contained in hemicelluloses present viable bio-substitutes for synthetic polymers across diverse applications [29] and demand, as such, refined extraction and modification protocols to harness their complete potential [29]. Moreover, due to their amorphous structure and reduced polymerization degree (relative to cellulose), hemicelluloses are, in general, more susceptible to chemical conversions than cellulose, which renders them suitable for an array of modification strategies [4]. In addition, their varied monosaccharide profile and branching motifs facilitate the synthesis of diverse functional biopolymers via chemical and enzymatic tailoring [30], [31]. These inherent characteristics and chemical adaptability position hemicelluloses as very promising substrates for conversion into bio-materials like hydrogels, films, and composites through chemical and biochemical modification routes [32]. These modifications (e.g., grafting of functional groups on the hemicellulose skeleton and/or side groups enzymatically or chemically) can, for instance, enhance their solubility, thermal resilience, and

mechanical performance, expanding their relevance in a broad range of material applications [30].

2.4. Hemicellulose extraction

Hemicellulose extraction has become an important aspect of biomass valorization, and a number of attempts have been made to develop and understand extraction techniques that could provide polymers with desirable purity, molar mass, and functional characteristics [22]. Traditional alkaline extraction remains one of the most widely applied approaches (primarily for the relatively alkaline stable xylan) because alkaline conditions efficiently dissolve hemicelluloses including also a partial cleavage of acetates and ester linkages to lignin, thus, liberating hemicelluloses from the lignocellulosic matrix [22], [30]. This method typically results in high yields and in some cases (xylan) only modest modification of the backbones, making them suitable for applications requiring larger molecular structures [21], [30]. However, under harsher conditions and especially in the case of glucomannans, alkaline conditions can alter the polymer structure, reduce branching by removing acetyl and uronic acid groups, or cause peeling reactions, which may reduce functionality for specific applications [20], [22], [32] Furthermore, alkaline extraction requires corrosion-resistant reactors and generates large volumes of chemical-rich effluent, posing challenges for both process design and environmental management [30], [32].

In contrast, hot-water extraction technique offers a more environmentally friendly route by avoiding harsh chemicals and relying primarily on hydrothermally driven conversion and solubilization under elevated temperatures and pressures [30]. Nevertheless, the increase of temperature to enhance solubilization can lead to partial depolymerization, dehydration reactions, and formation of degradation products such as furans and organic acids [3], [21]. This may compromise the molar mass distribution and functional integrity of the extracted hemicelluloses [21], [30]. Moreover, although hydrothermal methods reduce chemical consumption, they often require high energy input for maintaining pressurized systems, which affects industrial scalability and overall process economics due to equipment and energy costs [30], [32].

Emerging solvent-based technologies such as organosolv extraction, ionic liquids, and deep eutectic solvents (DES) present promising alternatives by enabling tunable extraction conditions and high-purity recovery [30], [32]. These solvents can disrupt lignin–carbohydrate complexes effectively while preserving the structural features of hemicelluloses, often yielding polymers with functionality suitable for films, hydrogels, and chemical modification [30]. For example, hemicelluloses extracted by organosolv methods can possess

high purity, with a structure similar to native hemicellulose [30]. DESs are also noted for their environmental friendliness, ease of preparation, and ability to achieve high recovery rates and structural integrity during extractions [30]. Yet, these methods still face considerable economic and environmental barriers associated mainly with difficulties to recycle the employed solvents, but in some cases also connected to toxicity, flammability, solvent costs, etc., hindering commercial application [30].

Consequently, the selection of an extraction technique must consider not only the quality and properties of the recovered hemicellulose but also the energy demand, environmental footprint, and cost effectiveness [22]. In the context of modern biorefineries, an integrated approach that aligns extraction performance with sustainability is essential for advancing hemicellulose-based materials [2].

2.5. Oxidation used for biomass valorization

Oxidation processes play an important role in modifying the structural and chemical properties of lignocellulosic biomass, enabling improved accessibility, reactivity, and functionality of its main components [16], [30], [33].

Hydrogen peroxide is widely used as an oxidative and bleaching agent due to its ability to oxidize and solubilize lignin under alkaline conditions [4]. It can be employed in alkaline oxidation processes to extract hemicellulose from biomass, leading to high purity and recovery rates of hemicellulose with low lignin content [30]. When performed under mild acidic conditions, hydrogen peroxide oxidation can also target carbohydrates, increasing carbonyl group content (through a radical mechanism) [34]. When applied to pulp, this oxidation can lead to a reduction in the water retention value and a substantial increase in wet web tensile strength, probably due to intra- and inter-fiber crosslinking of the introduced carbonyls.

TEMPO-mediated oxidation provides higher selectivity by converting primary hydroxyl groups of cellulose or hemicelluloses into aldehydes and carboxylates under mild conditions [16]. The introduction of carboxyl groups via TEMPO oxidation can increase solubility of hemicelluloses in water, which is critical for various applications [16]. The most famous use of TEMPO oxidation is, though, for selective surface carboxylation (charging) of cellulose microfibrils, promoting their disassembly into cellulose nanofibrils [35].

Periodate has emerged as a powerful and versatile oxidizer for polysaccharides due to its ability to selectively target and cleave vicinal diols, present in wood polysaccharides [33], [36], [37]. During the reaction, periodate cleaves the carbon–carbon bond between C2 and C3 of the anhydro-sugar units, producing two aldehyde groups, a transformation known

as the Malaprade reaction (Figure 4) [33]. It is possible to influence the yield of dialdehyde formation by adjusting reaction parameters such as time, temperature, and periodate concentration [36]. This allows for the modulation of the monosaccharide ring via cleavage of the diol structure and formation of aldehyde functionalities [38] which both helps disrupting hydrogen bonding networks and opens up for further conversions of the introduced aldehydes [33].

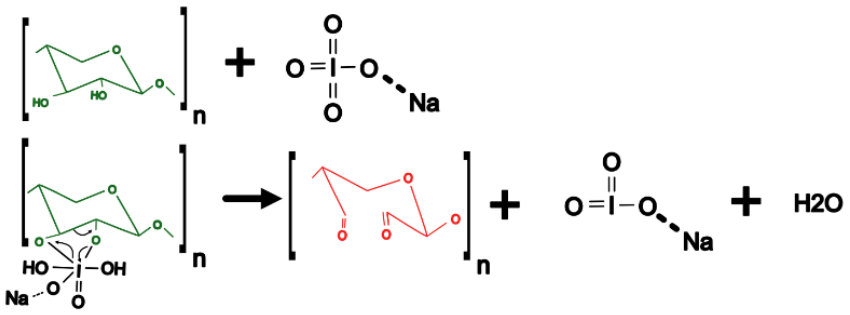


Figure 4: Periodate oxidation of xylan, forming two aldehyde groups, a transformation known as the Malaprade reaction

The resulting aldehydes can react with neighboring hydroxyl groups via intra- or intermolecular nucleophilic addition, forming cyclic or acyclic hemiacetal structures. Hemiacetal formation can occur within a single sugar unit, between adjacent residues along the same hemicellulose chain, or even between different polymer chains, potentially generating crosslinked networks [39]. More extensive oxidation can induce additional structural transformations. Double oxidation of susceptible sugar residues produces highly functionalized segments with multiple carbonyl groups, and intramolecular cleavage of already oxidized units may lead to rearranged carbohydrate fragments, which increases heterogeneity along the polymer backbone. Additionally, partial depolymerization can yield a mixture of oxidized oligo- and polysaccharides (with the introduced aldehydes partly further converted) combined with low-molecular degradation products.. Overall, periodate oxidation produces a dynamic ensemble of structures, including dialdehydes, hydrated aldehydes, hemiacetals, double-oxidized residues, and fragmented units (Figure 5), which collectively redefine the chemical architecture and reactivity of the original polysaccharides [39].

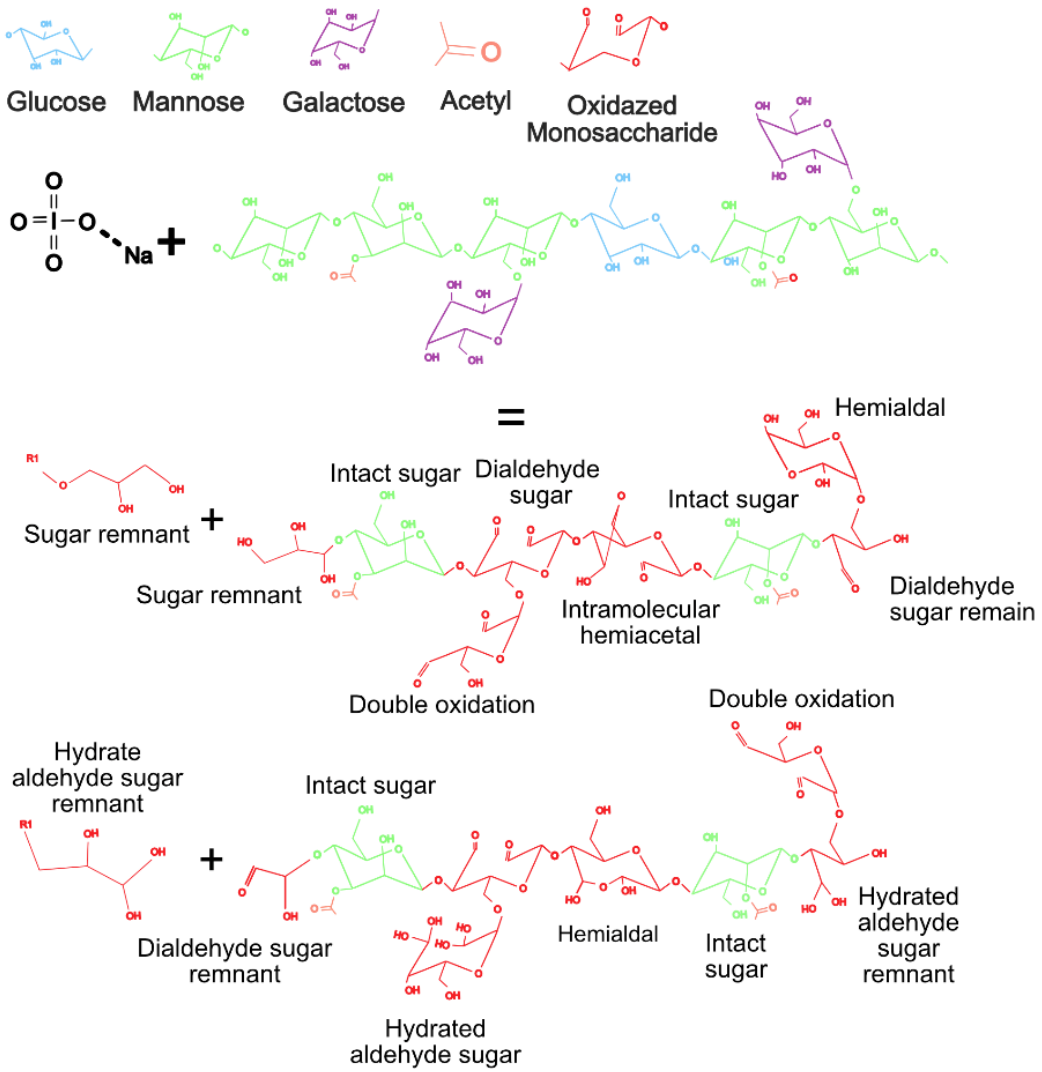


Figure 5: Periodate oxidation and its products and side products. Adaptation from [39].

2.6. Periodate use for extraction

Previous studies indicate possible influence of periodate oxidation (Figure 6) on the mobility and conformational flexibility of the hemicellulose backbone, particularly in xylan-based structures due to the ring opening effect [36], [40]. The oxidation reaction disrupts the tight packing and intermolecular bonding that normally stabilize the polymer [36], [40]. This structural change is expected to increase the rotational freedom of the remaining chain segments that could lead to a more flexible and mobile backbone [36], [40] with enhanced solubility or swellability in aqueous media [36], [38].

From an extraction perspective, the increased mobility and higher affinity for water offer important advantages, such as being more easily solubilized or separated from the lignocellulosic matrix. This suggests that periodate oxidation could serve not only as a modification technique but also as a pretreatment step to facilitate hemicellulose recovery, opening opportunities for more energy-efficient and selective extraction processes [16], [30].

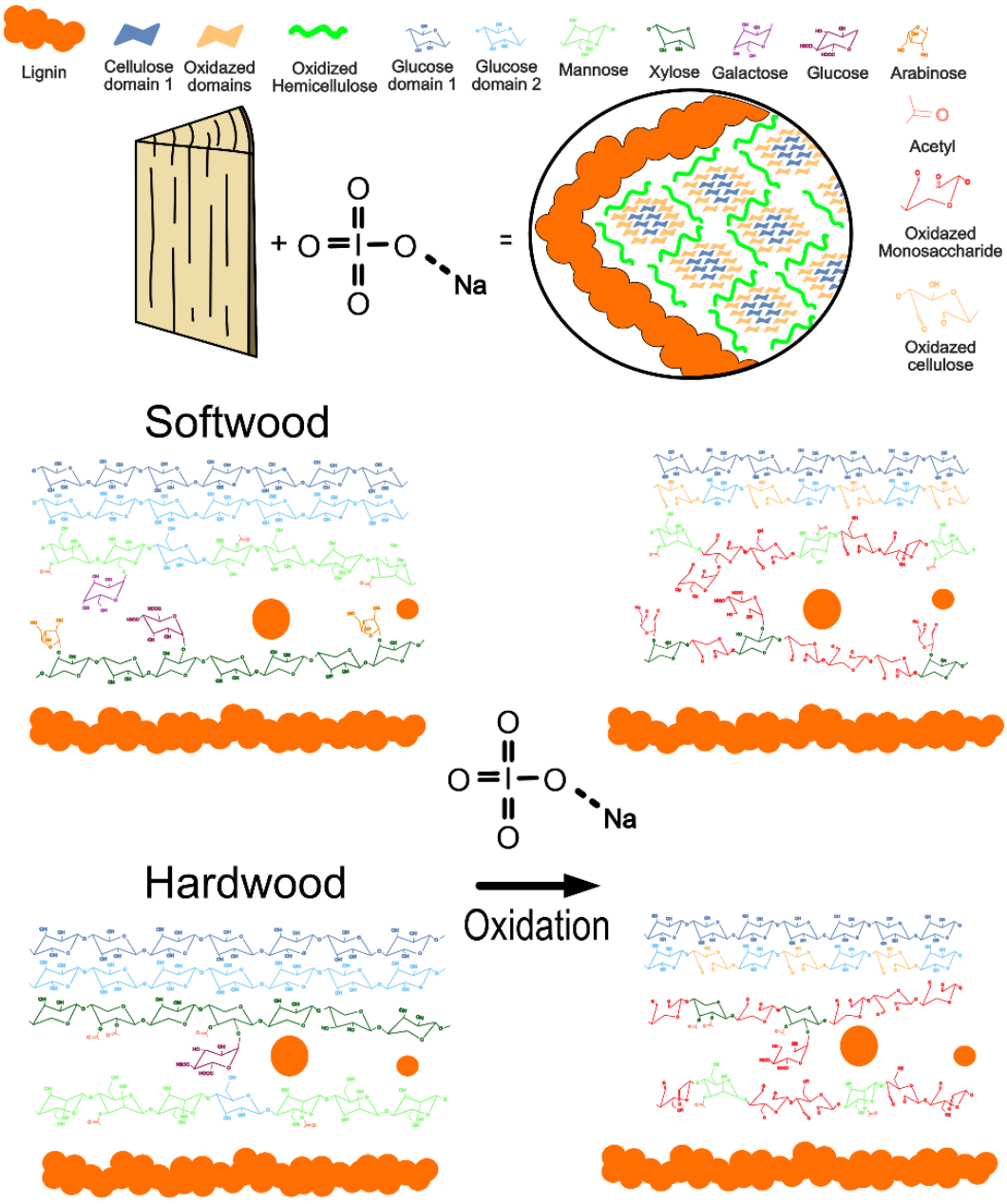


Figure 6: Schematic representation of softwood and hardwood after periodate oxidation (not to scale)

2.7. Modifications of the cell wall accessibility

2.7.1. Callose introduction

Compelling evidence establishes that cell wall architecture significantly governs accessibility of the cell wall polysaccharides to chemical reagents. The introduction of alternative polysaccharide structures, such as callose, into the plant cell wall of *Arabidopsis thaliana* has been shown to increase the distance between cellulose macrofibrils, thereby increasing porosity and potentially reducing biomass recalcitrance [41]. These architectural modifications substantially enhance the saccharification efficiency leading to sugar release increases of up to 53% for xylose and 25% for glucose andsignificant improvements in bioethanol production [41]. Such genetically induced enhancement of the cell wall accessibility suggests a potential to facilitate oxidative chemical modifications by improving reagent diffusion and substrate exposure, ultimately influencing processing kinetics, chemical consumption, and the properties of resulting material fractions. [41].

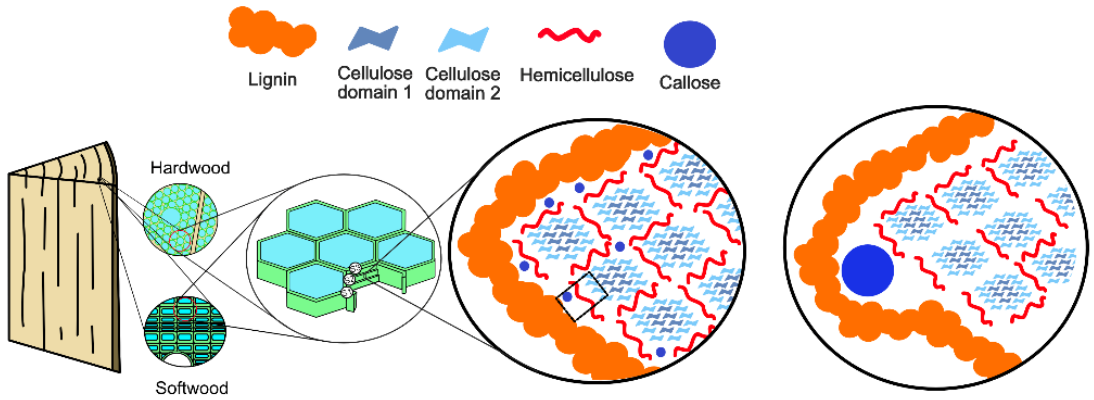


Figure 7: Schematic representation of the introduction of callose in the structure

2.7.2. Peracetic acid and delignification

Peracetic acid (PAA) treatment is an effective chemical method to selectively delignify lignocellulose, enhancing accessibility of carbohydrates in the cell wall (Figure 8) [7], [42]. As a powerful oxidizing agent, peracetic acid selectively attacks electron-rich lignin structures [43], [44] while preserving carbohydrates. It is particularly effective at cleaving βaryl-ether (β-O-4) linkages, which represent the most abundant interunit bonds in wood lignin polymer [7], [42], [44]. This oxidative cleavage significantly decreases the molar mass of lignin and introduces polar, oxygen-containing functional groups, specifically hydroxyl and carboxyl moieties (such as dicarboxylic

acids), thereby increasing lignin hydrophilicity and its subsequent solubility in aqueous media [7], [43], [44].

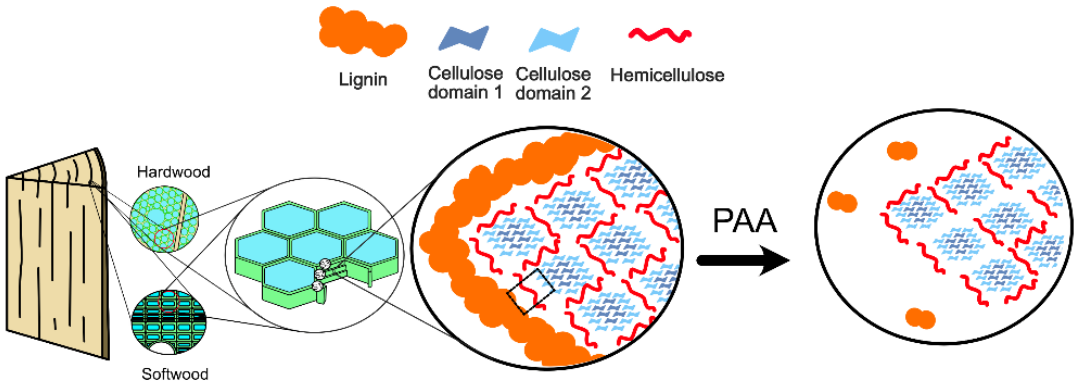


Figure 8: Schematic representation of the cell wall microstructure after PAA delignification

3. Materials and methods

The methods and materials described below have been basis for the work performed in the paper I (Study I) and Manuscript II (Study II).

3.1. Materials

For Study I Wood chips of birch (B), a hardwood, and spruce (S), a softwood, obtained from industrially cut logs, were screened to be free of bark and knots. For both studies, wood was milled separately with a knife mill and sieved into particles passing a 1-mm mesh.

For Study II, aspen biomass from two different wood sources was used: one wild (normal) wood and another genetically modified with 1% callose introduced into the structure [41]. The wood was milled to a powder state (1mm size). The samples were named as (A) aspen, (G) genetically modified, (W) wild aspen, (N) non-oxidized, (P) periodate oxidized, (L) lignified, and (D) delignified (Table 1).

Table 1: Summary of aspen samples with regard to, lignin content, and oxidation treatments.

Sample Code	Description	Oxidation Treatment	Lignin Status
AWNL	Wilds aspen	None (water)	Lignified
AGNL	Genetically modified aspen	None (water)	Lignified
AGND	Genetically modified aspen	None (water)	Delignified
AWPL	Wild aspen	$NaIO_4$ oxidation	Lignified
AGPL	Genetically modified aspen	$NaIO_4$ oxidation	Lignified
AGPD	Genetically modified aspen	$NaIO_4$ oxidation	Delignified

Hydroxylamine hydrochloride (H_2N-OH ·HCl), potassium Iodide (KI), sulfuric acid (H_2SO_4, 72%), sodium thiosulfate ($Na_2S_2O_3$), sodium hydroxide (NaOH), and sodium borohydride ($NaBH_4$), deuterium oxide (D_2O) were purchased from Sigma-Aldrich. $NaIO_4$ was purchased from ThermoScientific, and the ethylene glycol and dimethyl sulphoxide (DMSO) were purchased from VWR.

3.2. Delignification

For Study II, holocellulose samples were prepared according to the experiments described by Kumar [45]. In short, delignification was carried out by PAA in beakers containing 5 % (w/w) of dry solids, for 48h. At the end of the process, the slurry was vacuum filtered in a glass microfiber filter (Whatman GF/A 55 mm, Cytiva) and washed with distilled water (4× the volume of the slurry). Next, the solid residue was washed with a 50:50 (v:v) mixture of ethanol and acetone (2× the volume of the slurry). Then, the material was dried in an oven (40 °C) for four days and stored at room temperature inside a desiccator.

3.3. Sodium periodate oxidation

Sodium periodate oxidation was performed using both batch and flow-through configurations, depending on the objective of the experiment.

3.3.1. Oxidation as a function of time

Birch biomass powder and $NaIO_4$ were mixed in a mass ratio of 1:2 ($NaIO_4$:biomass) and suspended in deionized water at a solid-to-liquid ratio of 1:100 (w/v). The reaction was conducted in a 1-L reactor placed in a dark room to prevent light-induced side reactions with continuous stirring provided by a mechanical impeller to ensure homogeneous mixing. Aliquots of 70 mL were withdrawn from the reactor in time intervals of 2, 5, 10, 15, 20, 40, 60, 120, 180, and 240 min. After each sampling, the removed volume was immediately replaced with an equal amount of deionized water to maintain a constant reaction volume. Each aliquot was subsequently divided into four portions: 10 mL for carbohydrate composition analysis, quenched with ethylene glycol; 20 mL for aldehyde content titration; 20 mL for residual periodate quantification; and 20 mL subjected to reduction with sodium borohydride (10:1 $NaBH_4$:$NaIO_4$ molar ratio) in a sodium phosphate buffer medium (pH between 6.8 and 8), followed by dialysis using a 0.5 kDa molecular weight cut-off membrane (Spectrum Laboratories, USA) at a sample-to-water ratio of 1:20. The dialyzed fraction was then used for yield determination and molar mass distribution analysis by gel permeation chromatography (GPC) and Fourier transformation infrared spectroscopy (FTIR)

3.3.2. Oxidation as a function of oxidant charge

$NaIO_4$ and birch or spruce biomass were combined at varying mass ratios of [0:1], [1:4], [1:2], and [1:1] and suspended in deionized water at a solid-to-

liquid ratio of 1:100 (w/v). The mixtures were stirred continuously with a mechanical impeller for 1 h in a dark room to prevent light-induced side reactions. After the reaction period, each mixture was filtered using a Whatman® fiberglass microfilter to separate the solid and liquid phases. The solid residues retained on the filter were dried and subsequently analyzed for carbohydrate content and aldehyde and periodate content. GPC analyses were performed for $NaIO_4$-to-biomass mass ratios of 1:1, 1:2, and 1:4 to evaluate the molar mass distributions of the extracts under each oxidation condition. In contrast, Heteronuclear Single Quantum Correlation NMR (HSQC) analyses were conducted only for the [0:1] and [1:2] $NaIO_4$:birch mass ratios, which were selected as representative samples of the unoxidized reference and a moderately oxidized system, respectively.

3.3.3. $NAIO_4$ oxidation through flow reactor

Periodate oxidation was carried out in the laboratory developed flow-through reactor. A 1.0 wt% sodium periodate solution (1 g $NaIO_4$ in 100 mL water) was pumped through 2 g of dry biomass at a flow rate of 1.66 mL s^{-1}. The reactor effluent was collected in a container preloaded with ethylene glycol to immediately quench the reaction. Fractions were collected at time intervals of 0–20, 20–40, and 40–60 min. From each aliquot, one portion was used for hydroxylamine hydrochloride (H_2N–OH·HCl) titration and carbohydrate analysis, another portion was freeze-dried for NMR and GPC analyses, and the remaining fraction was dialyzed, using a 0.5 kDa molecular weight cut-off membrane (Spectrum Laboratories, Rancho Rodriguez, USA), at a sample-to-water ratio of 1:20. The dialysis water was exchanged five times. After dialysis, the samples were frozen and subsequently freeze-dried for 24 h. After the reaction, the residual solid biomass in the reactor was thoroughly washed with water and dried prior to further analysis.

3.4. Determination of aldehyde content

The aldehyde content was determined following a method adapted from Zhao and Hendel [46]. A 10-mL aliquot of the reaction liquor was diluted with 50 mL of deionized water, followed by the addition of 1 mL of 1 M H_2N–OH·HCl solution. The mixture was stirred for 40 min to allow the formation of oximes. After the reaction, the liberated HCl(aq) was titrated with 0.05 M NaOH(aq) using an automatic titrator (Titroline 7000, SI Analytics, San Diego, CA, USA)). The titration endpoint was set at pH 4.

3.5. Measurement of periodate consumption

The determination of residual periodate was performed based on the method described by Babor *et al.* [47]. A 10-mL aliquot of the reaction liquor was mixed with 1 mL of 1 M H_2SO_4 and 1 mL of 1 M KI, and the mixture was stirred for 1 h to allow a complete reaction (i.e. a complete consumption of the remaining periodate in the oxidation forming I_2). The liberated iodine was then titrated with 0.1 M $Na_2S_2O_3$ using a manual burette. Titration continued until the solution turned colorless, indicating the endpoint. A starch solution was used as an indicator to enhance the visual detection of the endpoint.

3.6. Carboxylic acid determination

The method was adapted from a method to quantify carboxyl groups in pulp using an autotitrator equipped with a pH electrode [48]. An aliquot of 25 mL of the reaction liquor was used directly for titration under magnetic stirring (300 rpm). Residual periodate was quenched prior to analysis using ethylene glycol. The titration was performed with standardized 0.01 M NaOH, starting from an initial pH of approximately 4 and proceeding until the solution reached pH 8.30, corresponding to the phenolphthalein equivalence point, where all carboxyl groups were neutralized. The autotitrator (Titroline 7000, SI Analytics, San Diego, CA, USA) operated in dynamic dosing mode, automatically reducing the NaOH addition step size near the endpoint to ensure accurate pH stabilization.

3.7. Yield

To determine the extraction yield, 20 mL of each extracted liquor sample was collected and dialyzed using a 0.5 kDa molecular weight cut-off membrane (Spectrum Laboratories, Rancho Rodriguez, USA) at a sample-to-water ratio of 1:20. The dialysis water was exchanged five times. After dialysis, the samples were frozen and subsequently freeze-dried for 24 h. The yield was calculated using Eq. 1, where m_f is the weight (g) of the container after freeze-drying, m_0 is the initial container weight (g), V_t is the total reaction volume (mL), V is the aliquot volume (mL) subjected to freeze-drying, and mt is the total mass (g) of biomass used in the reaction. To account for residual oxidant, an additional titration was performed on 1 mg of the freeze-dried sample to determine any excess periodate that was not removed during dialysis. The measured amount of residual periodate was subtracted from the calculated yield.

$$Yield\ (\%) = \frac{(m_f - m_0) \times V_t}{V \times m_t} \qquad (1)$$

3.8. Fourier transformation infrared spectroscopy analysis

For FTIR, 1 mg of each freeze-dried sample was homogenized with 120 mg of spectroscopic-grade KBr and pressed into pellets.
For Study I, samples obtained under condition B [1:2] were oxidized for 20, 40, and 60 min and analyzed by FTIR. To enable comparison with the NMR analysis of the 60 min samples (which were reduced with $NaBH_4$ to ensure solubility in D_2O; see the NMR sample preparation section below), these samples were also subjected to $NaBH_4$ reduction. After the oxidation, the reaction mixtures were filtered, and the filtrates were collected, adjusted in volume, concentrated, reduced with $NaBH_4$ (the procedure described above), dialyzed, and subsequently freeze-dried.
The solid residues remaining after extraction (wood) were thoroughly washed with deionized water, oven-dried at 50 °C, and finally freeze-dried. For comparison, an additional sample prepared under condition B [0:1] with a reaction time of 60 min was analyzed, along with untreated birch powder used as a reference material.
The FTIR spectra were recorded in transmission mode using a Frontier FTIR spectrophotometer (PerkinElmer Frontier, Waltham, MA, USA) over the range of 4000 to 650 cm^{-1}, with a spectral resolution of 4 cm^{-1}. For each sample, 16 scans were collected and averaged to improve the signal-to-noise ratio. All measurements were performed at room temperature.

3.9. Compositional analysis of obtained liquors and the solid residues

3.9.1 Neutral sugar analysis

The neutral sugar content of as well obtained extracts as residual solid material was determined by using high-performance anion-exchange chromatography with pulsed amperometric detection (HPAEC-PAD) as described below (Chromatography analysis of neutral sugars). For sample preparation from the extracts, 10 mL of the aliquots were mixed with ethylene glycol to quench the reaction. Acid hydrolysis was performed based in the procedure described by Sluiter [49] by adding 0.01 mL of 72% (w/w) H_2SO_4 to each sample, followed by autoclaving at 125 °C for 1 h. After cooling, 1.25 mL of 0.2 M fucose was added as an internal standard, and the solution was diluted to a final volume of 25 mL. Prior to analysis, 2 mL of each sample was filtered through 0.2-µm PTFE filters.
For sample preparation from the solid residues, 200 mg of the solid material (thoroughly washed after completed treatment) was subjected to total acid

hydrolysis following the procedure described above. Klason lignin content was determined gravimetrically measuring the solid residue after the total acid hydrolysis, following the procedure described by the National Renewable Energy Laboratory [49]. Carbohydrates were quantified analyzing the liquor fractions obtained after the total acid hydrolysis by anion exchange chromatography with pulsed amperometric detection (HPAEC-PAD, Dionex ICS-5000, Thermo Fisher Scientific, Waltham, USA). The system was equipped with a gold reference electrode and Dionex CarboPac PA1 columns (a 2 × 50 mm^2 guard column and a 2 × 250 mm^2 analytical column). The elution (dual pump: 0.26 mL/min and 0.13 mL/min) took place at 30 °C for 25 min using H_2O/200 mM NaOH, followed by a washing step of 13 min using 200 mM NaOH/200 mM NaOH + 170 mM sodium acetate. The injection volume was 10 µL. Data processing was performed using the Chromeleon software version 7.1.

3.9.2 Carbonyl content in the pulp

The total amount of carbonyl groups was determined using a method based on Zhao and Heindel [46] and described by Martinsson [34]. A never-dried pulp sample equivalent to 0.5 g of oven-dried pulp was dispersed in 100 mL of deionized water adjusted to a pH of 4. After 10 min, the suspension was filtered, and the sample was washed with 100 mL of deionized water at a pH of 4. The pulp was then transferred to a beaker containing 25 mL of 0.25 M hydroxylamine hydrochloride solution, also adjusted to pH 4. The mixture was placed on a shaking table for 2 h, after which it was filtered. The filtrate was titrated back to pH 4 using 0.01 M NaOH(aq). The pulp was subsequently washed with deionized water and dried in an oven at 105 °C for 24 h to determine the oven-dry mass. The total carbonyl content was calculated by determining the volume of the NaOH(aq) solution consumed during the titration, relative to the oven-dry weight of the pulp.

3.10. Gel permeation chromatography

For the Study I, after freez-drying, a solid sample of 1 mg for each studied condition was dissolved in DMSO overnight, diluted to 0.25 mg/mL, and filtered through a 0.2-µm filter. The molar mass distribution (MMD) of the samples was measured using gel permeation chromatography (PL-HPC 50 Plus Integrated GPC system (PI-GPC-50, Polymer Laboratories, Varian Inc., Agilent, Santa Clara, CA, USA). The system used two 300 × 7.5 mm^2 PolarGel-M columns and one 50 × 7.5 mm^2 PolarGel-M guard column. Dimethyl sulfoxide (DMSO) with 10 mM LiBr was used as the mobile phase, and the flow rate was 0.5 mL/min at 50 °C. Detection was made using an RI detector. The detector was calibrated with 10 Pullulan standards ranging from

0.180 to 708 kDa (Varian PL2090-0100, Varian Inc., Agilent, Santa Clara, CA, USA).
For Study II, after freezedrying the samples were prepares in a concentration of 10 mg/mL, and before injection, filtered (Acrodisc 13 mm syringe filter, 0.20 µm Nylon). A Tosho TSKgel GMPWXL column (7.8 × 300 mm, 13 µm) with a Tosho guard column (PWXL, 6.0 × 40 mm, 12 µm) and an inline filter (0.05 µm, Millipore VM) were used. The injection volume was 100 µL, and the flow rate was 0.5 mL/min. The HPLC system (Agilent 1260 Infinity II) included a degasser, quaternary pump, and autosampler. Detection was performed using an Optilab rEX refractive index detector. Data was analyzed with the ASTRA software (v7.3.2).

3.11. Nuclear magnetic resonance spectroscopy

Freeze-dried extract samples (10 mg) were dissolved in D_2O (0.30 mL) and analyzed by solution-state NMR spectroscopy. Spectra were recorded at 25 °C on a 600 MHz Bruker Avance III HD spectrometer equipped with a 3 mm TXO cryoprobe (600 MHz for ^{1}H, 150 MHz for ^{13}C). ^{1}H NMR spectra were acquired with 32 scans and a 1 s relaxation delay (Rheinstetten, Germany). HSQC spectra were recorded using pulse program hsqcedetgpsisp2.3, with acquisition times of 96 ms and 6 ms, respectively. The free induced decay (FID) sizes were 3072 and 512 points, respectively. The experiment consisted of 16 scans with a 1 s relaxation time, resulting in an experimental time of 3 h and 48 min. Data analysis was performed in Bruker TopSpin 4.1.4 software.

4. Results and discussion

To present the results and discussion in a clear and structured manner, this section is divided into three subsections. The first subsection examines the influence of reaction time on periodate oxidation and the subsequent extraction efficiency. The second subsection evaluates the effect of different periodate-to-biomass ratios, focusing on how reagent concentration affects oxidation performance and extraction behavior. The third subsection discusses the role of lignin in the process and how its presence influences both the oxidation reaction and the extraction results.

4.1. Oxidation effects on birch wood as a function of time

The selection of concentrations of periodate used in this part of the work was based on a range of previously reported studies Chemin *et al.* [37] Amer *et al.* [40], along with results from the preliminary experiments, point out that the mass ratio of 1:2 ($NaIO_4$:biomass) is a suitable starting point for investigating the effect of oxidation time applied. The extracts obtained after specific oxidation times were investigated in terms of yield, chemical composition (non-oxidized carbohydrates, aldehyde, and carboxylic acid content), and structure (molar mass distribution and presence of NMR-detectable structures). To enhance solubility required for the structural investigations (NMR and GPC), part of the obtained material was reduced with $NaBH_4$.

During the periodate oxidation of birch wood, the consumption of periodate exhibits a rapid initial phase, with approximately 40% of the oxidant being consumed within the first 20 min, increasing to 70% after 240 min (Figure 9a). This partial and time-dependent consumption is consistent with the behavior reported by Chemin *et al*. [37] for xylan, where incomplete oxidation was observed. For pure xylan, this observation was tentatively attributed by Palasingh *et al*. [38], and Zhu *et al*. [50] to the formation of inter- and intra-chain hemiacetal crosslinks, which can shield vicinal hydroxyls from further periodate attack, effectively “protecting” a portion of the polysaccharide from oxidation, as observed by Gomez *et al*. [51], Amer *et al*. [40], and Chemin *et al*. [37]. In wood material, on the other hand, both crosslinking reactions and the poor accessibility of the polysaccharide structures in general may contribute to a relatively slow consumption of the reagent.

The yield of extracted material (Figure 9b) increases over time, reflecting partial solubilization. At the same time, the generation of aldehydes in this material (as quantified by hydroxylamine titration (Figure 9c)) rises rapidly within the first 5 min, corresponding to the early periodate consumption. This increase is likely due to the formation of dialdehyde units along the

hemicellulose backbone, which may enhance chain flexibility and solubility, as observed by Börjesson *et al*. [36], Nishiyama *et al.* [52], and Nypelö *et al.* [33], but can also be associated with depolymerizing side-reactions promoting solubility. However, after this initial increase, the aldehyde concentration declines despite the continued presence of periodate, likely due to the above-mentioned crosslinking and accessibility issues hampering the oxidation and/or due to overoxidation to carboxylic acids as noted by Amer *et al.* [40], Pandeirada *et al.* [53], and Zhu *et al.* [50]. Indeed, as shown in Figure 9d, a progressive increase in carboxylic acid content could be observed during the oxidation of birch powder with $NaIO_4$ [54].

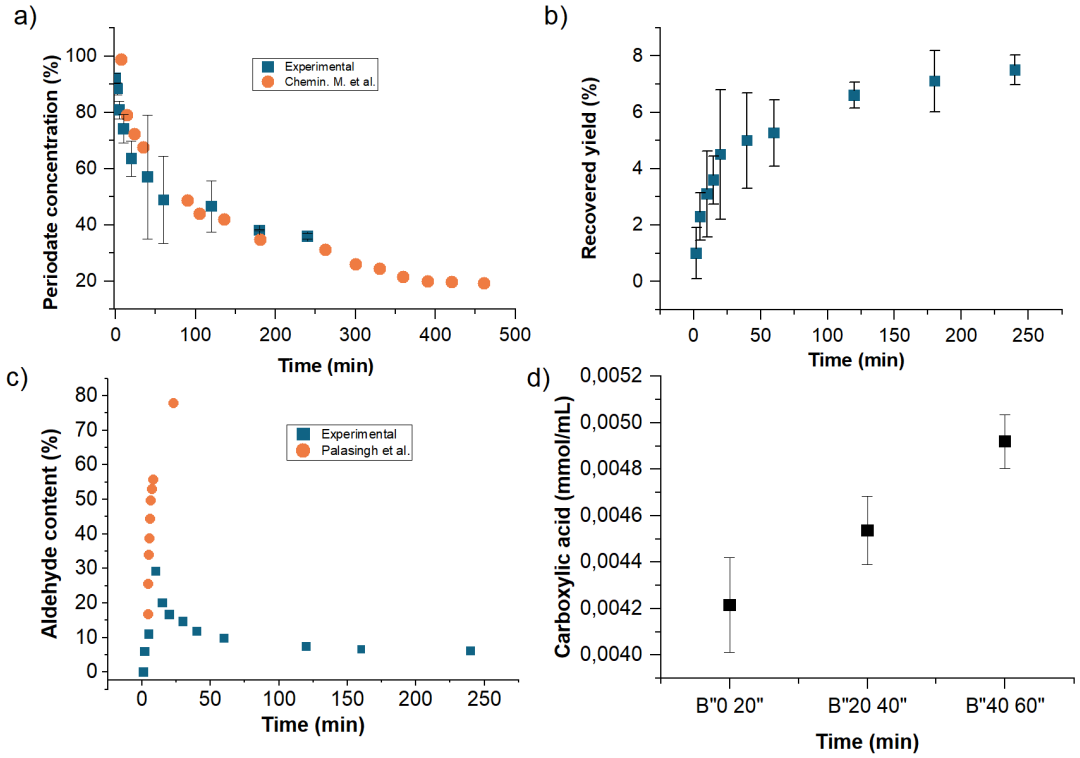


Figure 9: a) Periodate concentration (as % of total oxidizing liquor) during oxidation of birch, mass ratio 1:2 ($NaIO_4$: biomass) compared to the results obtained by Chemin M. *et al.*[37] ; b) yield of material extracted over the studied oxidation time; c) Aldehyde concentration detected in the extracted material (as % of the total dry mass over time compared to that obtained by Palasingh C. *et al*. [38]); and d) carboxylic acid amounts measured in extracted material over time for the same $NaIO_4$:biomass mass ratio.

In line with the observed formation of aldehydes, compositional analysis of the extracts in relation to the yield of extracted material over time (Figure 10), points out a consistent carbohydrate conversion (most likely through oxidation) throughout the extraction process. Within the first 2 to 5 min, approximately 50% of the extracted carbohydrates were converted and

undetectable as monosugars, increasing to 90% of undetectable monosugars in 60 min extracts. Beyond 240 min, the concentration stabilized, with more than 7% of the carbohydrates detectable. Glucose and xylose, which represented 78% of the recovered carbohydrates after 2 min of extraction, were both consumed to approximately 90% after 60 min and 95% after 240 min, respectively. Arabinose, which represented 12% of the recovered carbohydrates after 2 min of extraction, was consumed to 85% and 92% after 180 min and 240 min, respectively. These findings align with the previously reported results on the conversion of hemicelluloses by periodate oxidation [53].

Even though glucose typically accounts for no more than 5% of the hemicellulose fraction in birch [55], it constituted an important fraction of the extracted material, indicating a contribution from oxidative effects of periodate on cellulose. The latter can be associated with the mechanical milling the wood material was subjected to, increasing cellulose accessibility and susceptibility to oxidative and degrading chemistry of periodate [56], which (apart from a contribution from glucomannan and a probably minor presence of starch) could explain a significant presence of glucose in the extracts.

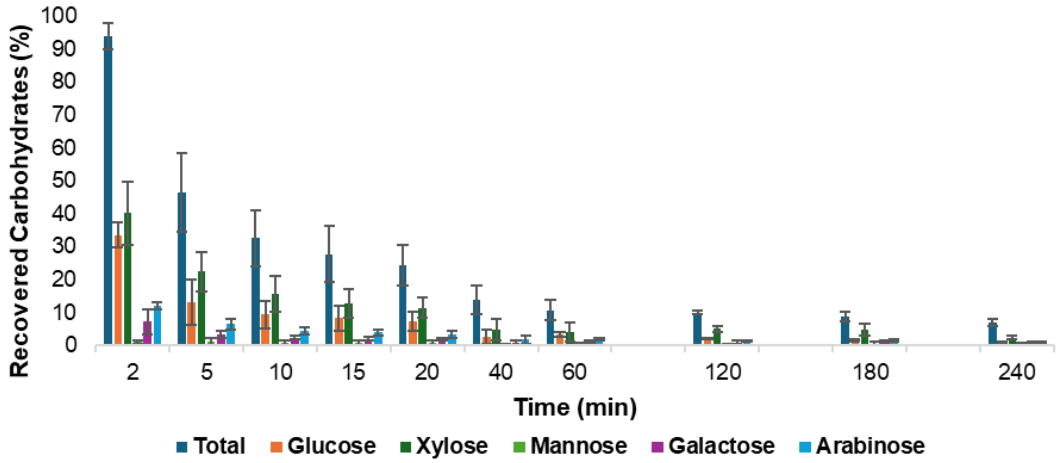


Figure 10: Carbohydrate concentrations (%) in the dry material of the liquor extracts over time in a birch treated with a 1:2 ($NaIO_4$: biomass) mass ratio; total concentration of detected carbohydrates in the extracted material is shown in dark blue.

Molar mass distributions (Figure 11) of the $NaBH_4$-reduced extracts show a bimodal distribution with a distinct, relatively narrow low-molecular fraction (corresponding to oligomer structures of DP ~5 to 11) and a broader, less abundant higher molecular fraction. Interestingly, the former increases over oxidation time, retaining rather constant molar mass, accompanied by a simultaneous shift of the latter towards lower molar masses. This behavior is

consistent with the previously observed depolymerization during periodate oxidation [53], demonstrating that periodate oxidation generates distinct oligomers formed at branching positions within the polysaccharide. These branch-points inhibit continued cleavage, resulting in stable fragments of characteristic size. For birch wood xylan, Pandeirada *et al.* [53] observed release of oligomers of DP 2-20 even at room temperature, and Fliri *et al*. [57] confirmed that depolymerization begins early during periodate oxidation, even at low to moderate degrees of oxidation. Similarly, Chetouani *et al*. [58] reported formation of a low-molecular fraction during prolonged periodate oxidation of pectin. In our study, the biomass extracts comprised rather complex mixtures of oxidized poly- and oligosaccharides where the alkaline reduction associated with β-elimination during the $NaBH_4$ reduction likely additionally affected molar mass of the extracted carbohydrates. Thus, while it is possible that the observed low molecular fraction indeed is characteristic of the main polysaccharide degrading during this treatment (possibly xylan, (Figure 10)), further investigations are required, particularly those focusing on revealing characteristic residual oligosaccharide from the periodate degradation of native xylan.

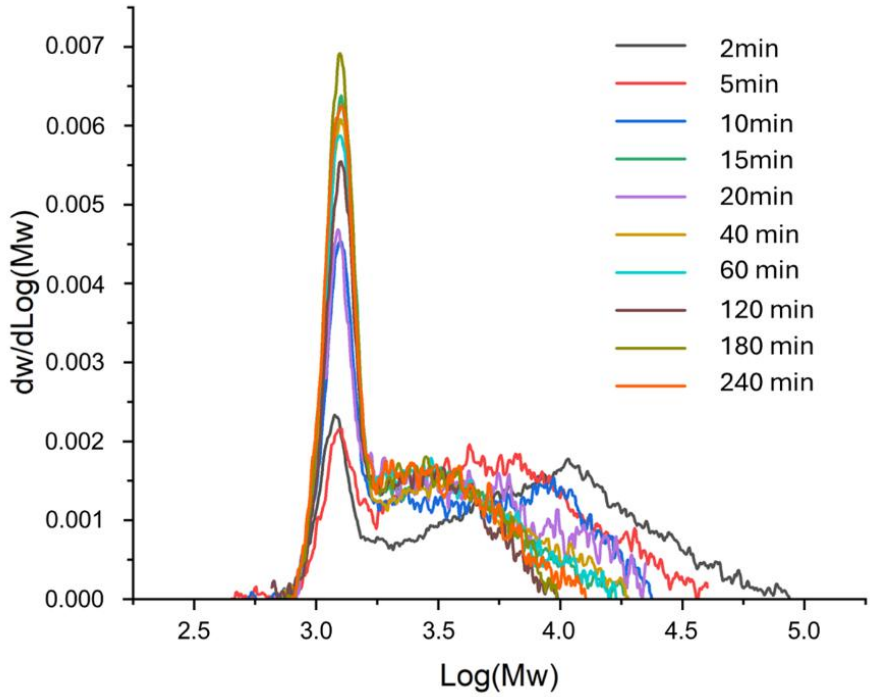


Figure 11: Molar mass distribution of the extracted and reduced material obtained after different oxidation times (0 to 240 min) while treated with the ratio 1:2 ($NaIO_4$:biomass).

Compared to the HSQC spectrum of the reference water-extract (Figure 12a)(with no oxidation involved, sample B [0:1]), which displays resonances

characteristic of water-soluble polysaccharides and phenolic compounds. The HSQC spectrum of the periodate extract from the 1:2 ($NaIO_4$:biomass) (Figure 12b), sample treated for 60 min shows a mixture of signals originating from oxidized and unoxidized carbohydrate structures. In addition to the above-mentioned signals of the unoxidized sugars, a distinct cross-peak at δH ~4.8 / δC ~90 ppm is attributed to hemiacetals [59] or anomeric-like carbons adjacent to C1 affected by oxidation [60], [61]. Weak resonances at δH 1.2 to 1.5 / δC 14 to 30 ppm indicate aliphatic methylene chains, which may originate from oxidative degradation products [60]. Additional peaks at δH 2.0 to 2.2 / δC ~20 ppm confirm the presence of acetyl substituents in birch xylan, demonstrating retention of O-acetylation following the oxidation treatment [18], although the extent to which the O-acetylation is preserved remains unclear.

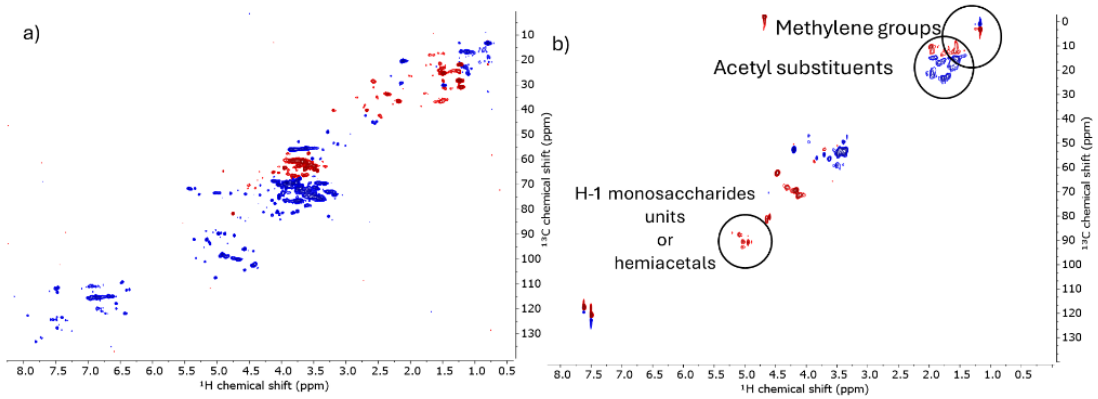


Figure 12: ^{1}H-^{13}C HQSC NMR spectra of birch for a) reference water-extracted sample for 60 min and b) periodate extracted sample after treatment for 60 min, 1:2 ratio ($NaIO_4$:biomass). Red and blue contours represent signals with positive and negative phases, respectively, corresponding to CH/CH_3 and CH_2 groups in the multiplicity-edited HSQC experiment.

The complementary FTIR analysis of the liquors obtained after birch oxidation and subsequent reduction (Figure 13a) reveals several characteristic bands associated with structural changes in the polysaccharide matrix [62] such as the band in the region1637 to 1650 cm^{-1} corresponding mainly to the bending vibration of absorbed or bound water (H–O–H) and the contribution at 1610 cm^{-1} assigned to the asymmetric stretching of carboxylate groups (COO^-). The persistence of the 1610 cm^{-1} signal after $NaBH_4$ reduction indicates that carboxyl groups, formed during oxidative cleavage of polysaccharide chains, remain unaffected by the reducing agent, which selectively reduces aldehydes but not acids. In contrast, the absorption band at 1740 to 1750 cm^{-1}, indicative of hemicellulose acetates, could be observed only in the

reference (water) extract, probably as the acetates were hydrolyzed off during the $NaBH_4$ reduction of the periodate extracted samples. In the solid residue (not subjected to the reduction), these bands could be observed both after water- and periodate-extraction (Figure 13b).

In the 1430 to 1380 cm^{-1} region, the observed bands are attributed to C–H stretching and bending modes of methylene groups ($–CH_2–$) [63]. Their increased relative intensity following reduction is consistent with the conversion of aldehyde groups to primary alcohols ($–CH_2OH$), confirming the reduction of dialdehyde intermediates. A diffuse band near 850 to 890 cm^{-1} is assigned to C–C or C–O skeletal vibrations of the pyranose ring and to the presence of hemiacetal and hydrated forms, characteristic of periodate-oxidized carbohydrates [64].

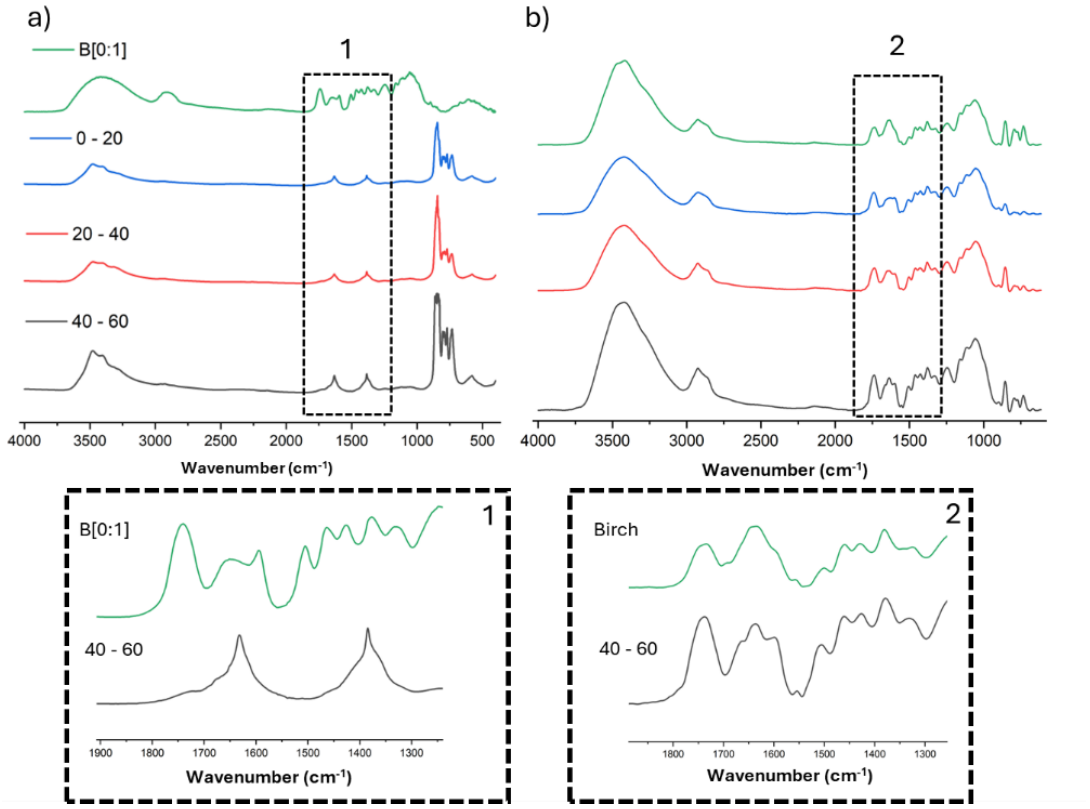


Figure 13: FTIR spectra of a) liquor samples extracted with only water (B[0:1]) and periodate ($NaIO_4$:biomass ratio 1:2) for different treatment times (0 to 60 min), followed by $NaBH_4$ reduction; b) the remaining solid fractions.

4.2. The impact of periodate concentration and type of biomass on the effects of oxidation/extraction

To gain an insight in the impact of biomass and periodate charge on the outcome of extraction, birch and spruce were treated with varied periodate

concentrations for 1 h – the length of the treatment that would, according to the results showed above, allow for relatively high extraction yields and aldehyde generation (Figure 9b-c), while limiting the degradation reactions (Figure 11). In Figure 14a, the consumption of periodate after 60 min of oxidation of birch and spruce is presented for different periodate concentrations. In all cases, more than 50% of the oxidant was consumed within this period. As shown in Figure 14b, the extraction yield calculated relative to the initial biomass input increased with higher periodate dosages, indicating a positive correlation between oxidant loading and material extractability. Aldehyde formation and recovered yield are also reported in Figure 14b.

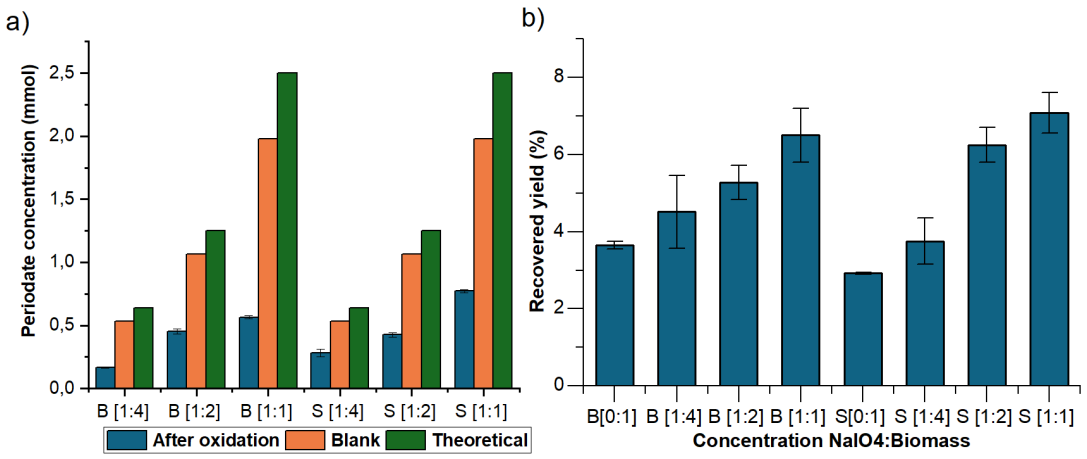


Figure 14: a) Periodate consumption during oxidation of birch (B samples) and spruce (S samples) for different oxidant charges ($NaIO_4$:biomass mass ratios), b) Yield of material recovered for different oxidant charges.

Although attributing the oxidation effects to individual monosugars is difficult in this work, Figure 15a indicates extracted monosugars resistant to periodate oxidation. Xylose in birch seems to be affected only to a relatively low extent by oxidation, as xylose levels in extracts only modestly vary with periodate concentration, even when comparing the water to periodate extraction. This is especially prominent when compared to the quite drastic decrease in glucose concentration as the periodate charge is increased. These very different behaviors might be explained by the relatively high level of acetylation of the birch xylan [65], preventing oxidation by blocking access to the vicinal alcohols (in C2 and C3). Glucose, on the other hand (in cellulose and glucomannan), is unsubstituted, allowing for more extensive oxidation through reaction of available vicinal alcohols [65]. The concentrations of both

monosugars decrease with increasing periodate loading, dropping from 37% to 12% and 7% at the B[1:2] ratio, and further to 5% and 3% at the B[1:1] ratio, respectively, when compared with the B[0:1] reference sample.
In line with this, in spruce, where the hemicelluloses are primarily composed of galactoglucomannan (galactose, glucose, and mannose, with acetylation on mannose) and some xylan carrying 4-O-methylglucuronic acids (and no acetylation), lower amounts of unoxidized sugars could be detected, possibly indicating a higher degree of oxidation that might be associated with a higher content of unsubstituted hexoses (even though some positions in mannose are substituted by galactose or acetates) and pentoses (non-acetylated xylan) with available vicinal hydroxy groups. In these experiments, the degree of oxidation was varied by adjusting the sodium periodate to biomass mass ratio (S[1:2], S[1:1], and S[0:1]). After oxidation, the concentrations of hexoses were reduced to 6%, 8%, and 5% at the S[1:2] ratio, and to 4%, 3%, and 3% at the S[1:1] ratio, respectively, compared with the S[0:1] reference sample.
Following the decreasing amounts of non-oxidized monosugars, the formation of aldehydes in extracts increases with the increasing periodate charge (Figure 15b). However, the aldehyde concentration does not consistently correlate with the decrease in monosugar content, particularly at higher periodate levels, where it declines despite the continued reduction in detectable monosugars, indicating ongoing oxidation. This behavior suggests that extensive oxidation promotes competing side reactions, including aldehyde degradation as reported by Pandeirada *et al*. [53], crosslinking reactions reducing their accessibility to the titrating agent [57], and overoxidation to carboxylic acids (Figure 9d), previously also observed by Zhu *et al*. [50]. Therefore, the measured aldehyde content may not increase proportionally with the periodate dosage or reaction time, as some aldehydes are lost or inaccessible.
Carbohydrate composition of the residual solid material reflects these extraction trends, showing a decrease in carbohydrate content for both birch and spruce as periodate charge is increased (Figure 15c).
Even aldehyde generation in the solid material follows the same trend (Figure 15d), confirming that the oxidation affects not only the extracted materials but also the solid residue. These aldehydes arise both from the oxidation of exposed vicinal diols in the glucose units of cellulose and from modifications of hemicelluloses retained in the structure. Just as observed in the corresponding liquors, aldehyde content in the solid material increases up to the [1:2] $NaIO_4$:biomass ratio, after which a further increase in oxidant dosage results in a decline in measurable aldehyde concentration due to the above-discussed side reactions leading to inaccessibility or removal of aldehydes. Moreover, the amount of detected Klason lignin in the solid residue increases

with increasing periodate charge (Figure 16), probably primarily indicative of the increasing introduction of oxidized groups to carbohydrates that during the total acid hydrolysis (involved in the Klason lignin determination) contribute to formation of condensed insoluble (crosslinked) structures detected in the solid Klason lignin fraction (pseudo lignin) [66], [67], and reported in previous studies in the field [37], [40], [50], [53].

Evidently, hemicellulose response to periodate oxidation differs between hardwoods and softwoods due to variations in hemicellulose structure and probably also cell wall architecture (which was not approached in this work). In birch, the dominant hemicellulose is a rather heavily acetylated O-acetyl-4-O-methylglucuronoxylan (with on average 4 acetates per 10 xylose units [18]) with less vicinal diols accessible to periodate oxidation [20], [33]. In contrast, spruce hemicelluloses are primarily galactoglucomannans, which are comparably less substituted (with a typical Man:Glc:Gal ratio in Norway spruce being 3.5 to 4.5:1:0.5 to 1.1 and 2 to 3 acetates per 10 mannose units [19], [68]) and as such might offer a higher amount of vicinal diols available for oxidation [38].

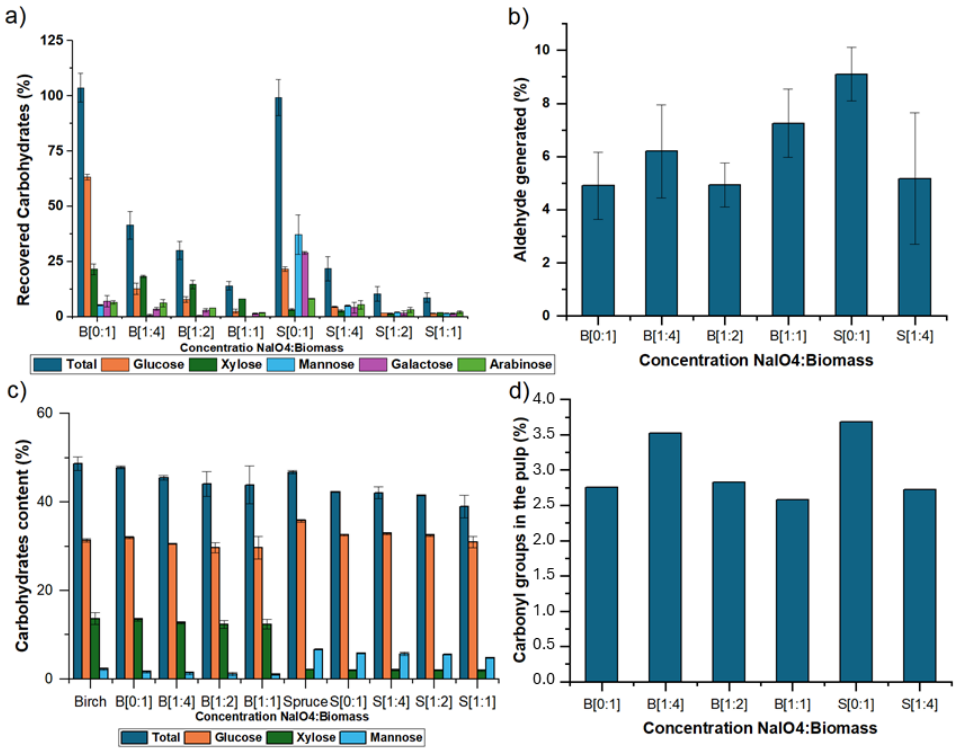


Figure 15: a) Recovered extracted carbohydrates as % of the dry total extracted material for different periodate: biomass mass ratios after 60 min, for birch and spruce; b) Aldehyde generation as % of the total dry mass of the liquor extracted; c) Amount of carbohydrates in solid material recovered after extraction as % of the total dry mass of detected carbohydrates for different periodate: biomass mass ratios after 60 min, for birch and spruce, total amount of extracted carbohydrates as % of the total dry

mass is shown in dark blue; d) Aldehyde concentration detected in the extracted material (as % of the analyzed dry pulp).

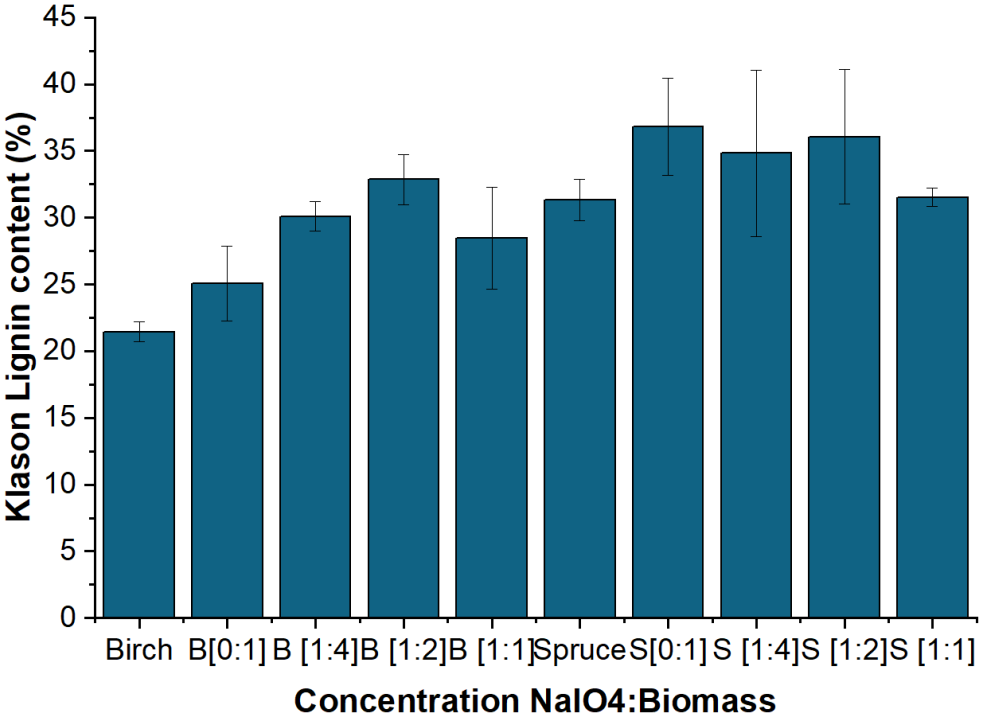


Figure 16: Klason lignin concentration detected in the solid residue expressed as % of the dry content for different periodate charges after 60 min treatment, for birch and spruce biomass.

The influence of the various periodate oxidation conditions on the MMD of polysaccharides was studied by GPC (Figure 17). All aliquots contained structures within a degree of polymerization in agreement with other studies [37], [53]. Also, in agreement with Pandeirada *et al*. [53] and Fliri *et al*. [57], the increase in periodate concentration extends the depolymerization.

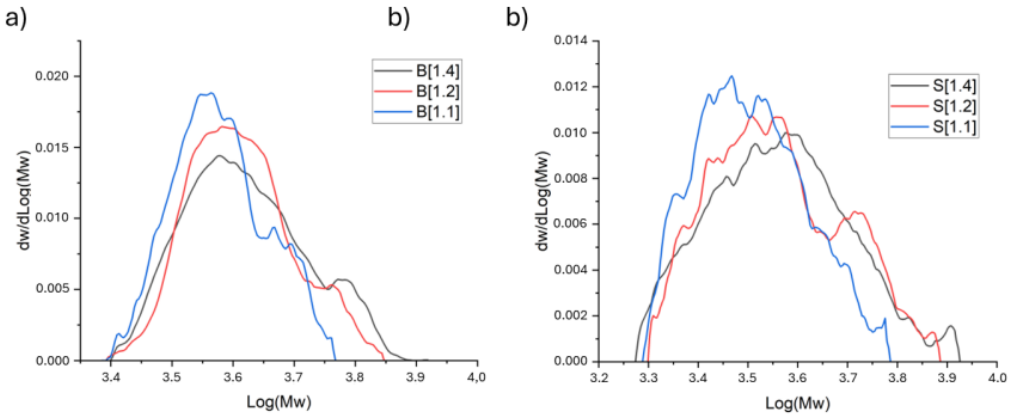


Figure 17: a) Influence of periodate concentration on molar mass of the extracted material upon oxidation of birch, b) Influence of periodate concentration on molar mass of the extracted material upon oxidation of spruce for 60 min.

4.3. Impact of cell wall accessibility on the oxidative extraction

In the work presented below, the effects of cell wall modification (through removal of lignin and/or introduction of a spacer between cellulose fibrils in aspen) on the outcome of periodate-mediated extraction have been investigated. Lignin removal has been carried out through the commonly used peracetic acid delignification [42], [69], while introduction of a spacer between cellulose macrofibrils has been accomplished through genetical modification of aspen [41] rendering interfibrillar introduction of callose reported to enhance porosity of the cell wall [41]. Both of these modifications of the cell wall accessibility were expected to enhance oxidative extractions from the cell wall.

From Figure 18, it is evident that periodate oxidation significantly promotes extraction compared to water; however, neither lignification of the biomass nor spacing of cellulose macrofibrils appear to have a substantial effect on the overall extraction yield (at least for structures above 500 Da). A slightly higher yield is observed for the callose-rich delignified wood at early time points (0–20 and 20–40 min), although this effect is modest and not consistently pronounced.

Samples obtained by the periodate-mediated extraction presented an initially relatively high yield, which further increased during the 20-to-40-minute extraction period. Between 40 and 60 minutes, the amount of extracted material drastically decreased in all cases. This might be partly attributed to the exhaustion of the extractable material, but is also likely a consequence of the extensive depolymerization induced by the oxidation process [33], [36],

[37] leading possibly to a significant extraction of undetectable low-molecular material (below 500 Da), which is removed during the dialysis purification.

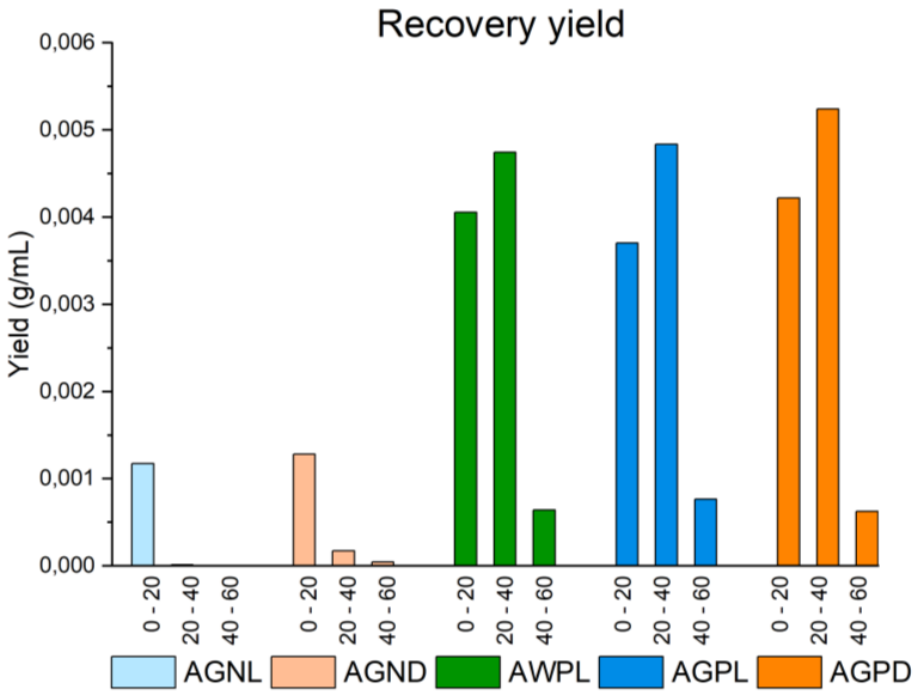


Figure 18: Figure 1: Recovered yield over 500Da in aliquots collected at 0–20, 20–40, and 40–60 min of the extraction. A = aspen; W = wild (normal) aspen; G = genetically modified aspen; P = periodate oxidized; L = lignified; D = delignified.

The extracted material is composed of both oxidized and non-oxidized structures, originating predominantly from wood carbohydrates. Non-oxidized carbohydrate content of the obtained extracts is shown in Figure 19. Water extracts from the lignified samples are very similar in their composition regardless of the callose-spacing (AWNL and AGNL) and contain mainly glucose. Similar behavior of these samples is observed even upon periodate oxidation, characterized by an increase in glucose release compared to water extraction.

Interestingly, though, the employed delignification seems to provide access to xylan both for the water and periodate-mediated extraction, as all the extracts from delignified samples – whether extracted by pure water (AGND) or through periodate-mediated procedure (AGPD) - show a significantly higher carbohydrate recovery dominated by xylan compared to the lignified counterparts. Upon oxidation (AGPD), even higher extraction yield (and more xylose) is obtained, while simultaneously showing a lower galactose content compared with the water-extracted reference (AGND).

The increased amount of non-oxidized carbohydrates recovered from delignified material suggests that lignin plays an important role in anchoring hemicelluloses within the cell wall during the oxidation-mediated extraction, making it less accessible to periodate due to both covalent bonding with lignin and physical entrapment [7], [33]. For that reason, the PAA-delignification facilitates greater polysaccharide release by increasing the overall accessibility of the carbohydrate chains to the oxidant [7], [43], [69]. The PAA delignification is, namely, recognized for its efficient lignin removal by selectively targeting aromatic and benzylic structures, promoting the cleavage of aryl-ether bonds, reducing lignin molar mass, and introducing hydrophilic functional groups that enhance solubility [42], [70], [71]. Importantly, the benzylic α-carbon in lignin side chains is particularly susceptible to oxidative attack, and some lignin–carbohydrate complexes (LCCs) are suggested to be linked linked through this position [25]. As a result, oxidative cleavage at the α-position may contribute directly to the disruption of the LCC linkages. Moreover, sodium periodate oxidation also targets vicinal diols in carbohydrate structures adjacent to the same α-position. This overlap in reactivity may further promote the cleavage of lignin–hemicellulose linkages and facilitate the release of hemicellulose chains [25], [72]. Consequently, the PAA treatment partially disrupts lignin–xylan connectivity, increasing the exposure of glucuronoxylan without extensive depolymerization [7], [69], [73], [74]. This enhanced accessibility facilitates subsequent chemical modifications such as sodium periodate oxidation.

However, the efficiency of periodate treatment is also intrinsically limited by structural features of glucuronoxylan. In hardwood xylans, acetyl substitutions at the C-2 and/or C-3 positions block the vicinal diols required for periodate oxidation [18], [75], restricting probably reactivity to deacetylated regions of the xylan backbone [61], [76].

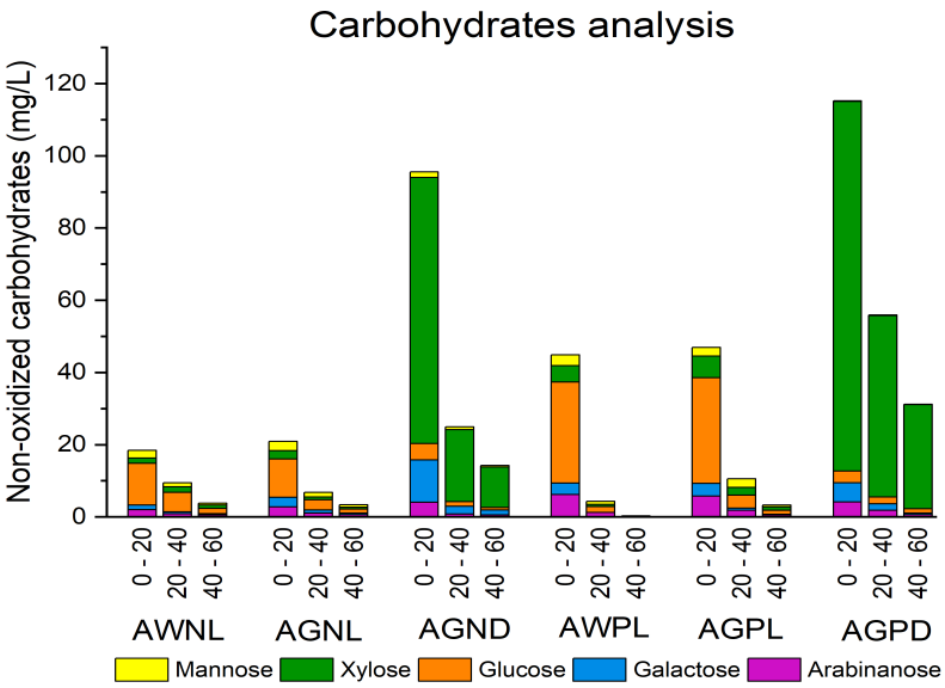


Figure 19: Concentration of recovered non-oxidized carbohydrates (mg/L) in 5 mL aliquots collected at 0–20, 20–40, and 40–60 min of the extraction. A = aspen; W = wild (normal) aspen; G = genetically modified aspen; N = water-treated; P = periodate oxidized; L = lignified; D = delignified.

While the composition of the obtained extracts was strongly influenced by biomass lignification (with xylan being predominantly recovered from the delignified material), the content of detectable aldehydes remained surprisingly similar across samples with varying accessibility (Figure 20). This observation raises the question of how much of the total carbohydrate content is intrinsically available for aldehyde formation, independent of structural barriers/spacers such as lignin or callose. The periodate oxidation specifically targets free vicinal diols at the C2–C3 positions of xylopyranose units[57]. However, in native hardwood xylan, approximately 40–70% of these positions are blocked by O-acetyl substituents [75], leading to a heterogeneous and limited formation of dialdehyde functionalities [57], [77], as only the deacetylated regions are susceptible to oxidation [78]. In Figure 20, aldehyde generation has reproduced the behavior noted in Figure 9c, showing an initial increase in aldehyde formation followed by reaching a plateau despite the continued presence of periodate. This was likely due to the above-mentioned crosslinking (and the accompanying accessibility issues) hampering the oxidation and/or due to overoxidation to carboxylic acids, as noted by Amer *et al*. [40], Pandeirada *et a*l. [53], and Zhu *et al*.[50]

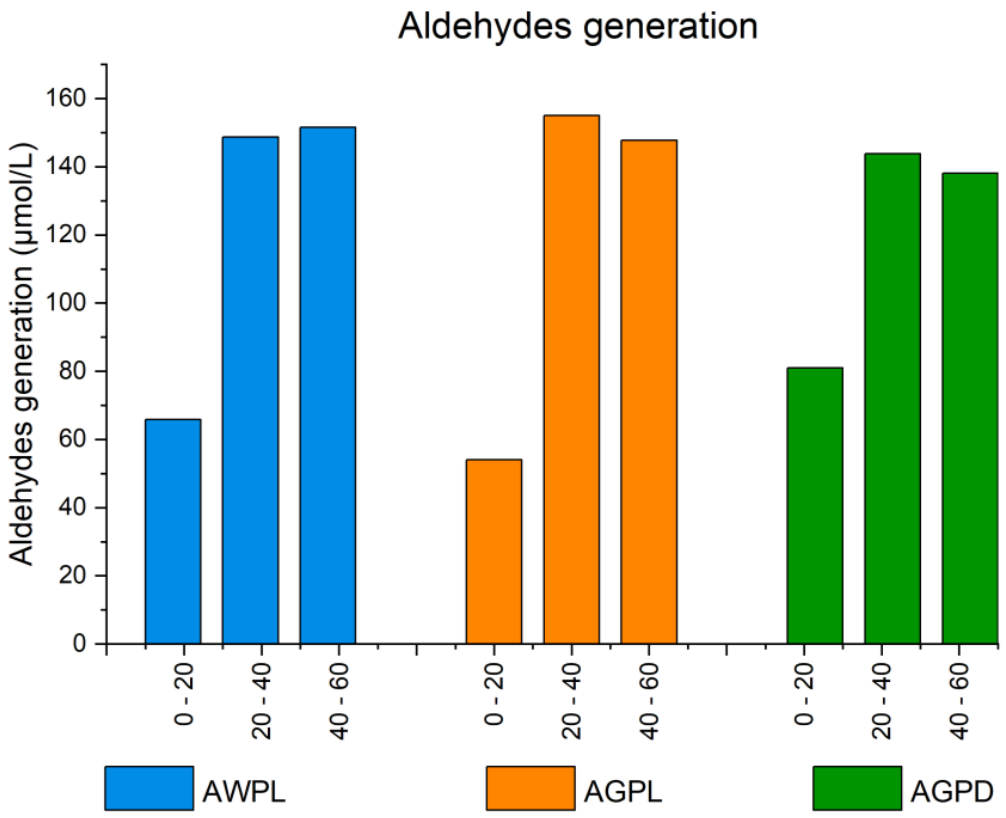


Figure 20: Aldehyde concentration (µmol/L) detected in aliquots collected at 0–20, 20–40, and 40–60 minutes of the extraction. A = aspen; W = wild (normal)aspen; G = genetically modified aspen; P = periodate oxidized; L = lignified; D = delignified.

Interestingly, while removal of lignin significantly affects the molar mass distribution of the structures extracted with pure water (e.g.the lignified samples generate water extracts in the range 1000-10000 Da shifting to significantly higher molar masses centered around 24 000 Da after delignification), the extracts obtained through periodate oxidation show very similar molar mass distributions regardless of the lignification/modification of the biomass (Figure 21). The former can be explained by increased exposure of water-soluble structures (predominantly hemicelluloses) to the aqueous environment upon lignin removal [73], including also substantial cleavage of linkages between hemicellulose and lignin [24], [78], [79], allowing larger polymeric fragments to be released into solution [24], [73]. The latter (i.e. molar mass distributions obtained upon periodate oxidation), on the other hand, is strongly indicative of the degrading nature of periodate treatment and is in line with our previous findings. The periodate is known to cause a substantial decrease in the molar mass of polysaccharides, turning them often into soluble oligosaccharides, with the extent of depolymerization

increasing with higher oxidant ratios [40], [53], [80]. For instance, after exposure to periodate for 20 minutes, the lignified samples showed a substantial decrease in molar mass compared to corresponding water extracts, with all detected species being below 1500 Da. Yet, after the same extraction time (20 min), the extracts from the delignified samples still exhibited a small fraction with molar mass around 10 kDa. This suggests that the presence of lignin can limit hemicellulose dissolution during periodate oxidation. However, upon longer exposure, 40 to 60 minutes, all the recovered carbohydrate fractions decreased to molar mass below 1500 Da.

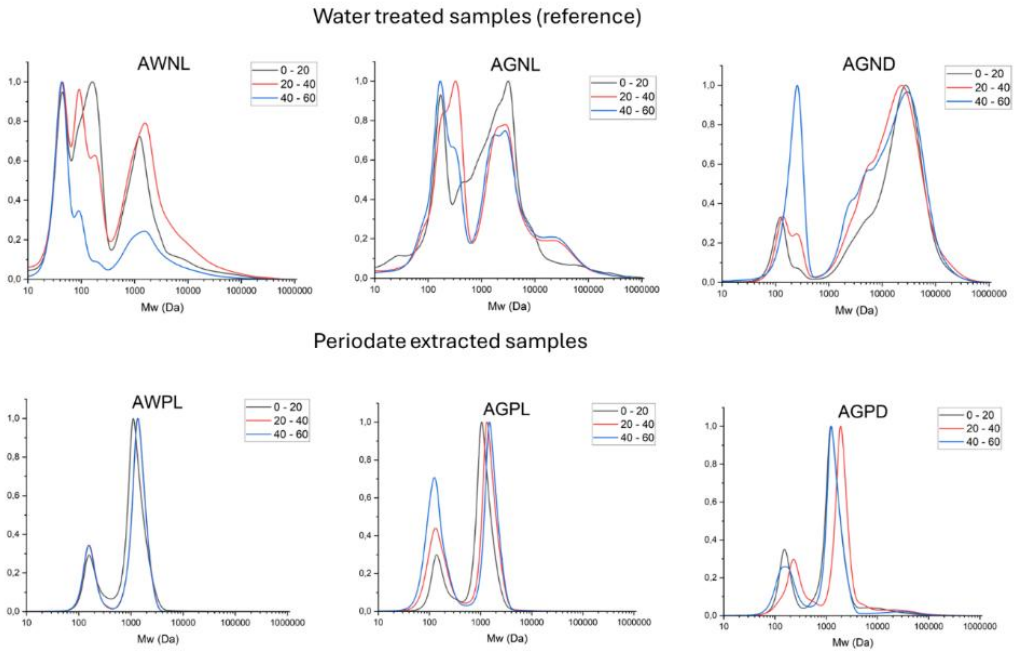


Figure 21: Molar mass distribution (Mw, Da) of dissolved fractions collected at 0–20, 20–40, and 40–60 min of the extraction. A = aspen; W = wild (normal) aspen; G = genetically modified aspen; N = water-treated; P = periodate oxidized; L = lignified; D = delignified.

In Figure 22, the ^{1}H NMR spectrum of the aqueous extract obtained from lignified aspen biomass (AGNL) is dominated by broad carbohydrate resonances in the 3.0–5.5 ppm region, which corresponds to protons attached to oxygenated carbons in cellulose and hemicelluloses [40], [81], [82], with the anomeric protons (H-1) appearing [40], [82]between 4.4 and 5.2 ppm for soluble oligosaccharides [40], [82].

In addition, peaks between 0–3 ppm are related to methyl aliphatic structures [60] (the peak at 2 ppm is indicative of the acetylated hemicellulose structures) [18], [83]. Peaks between 6 and 9 ppm are associated with aromatic protons, characteristic of lignin-derived structures solubilized during water extraction [84]. As expected, these signals strongly decrease upon

delignification [85], while the signals corresponding to anomeric protons (at approximately 4.4 ppm), and those around 3.6 and 3.55 ppm, attributed to C-6 methylene protons suggests a higher presence of soluble carbohydrate fragments, after lignin removal [86]. The peaks related to the methyl signal near 2.0–2.2 ppm also increase, possibly resulting from the hemicellulose acetyl groups and/or the presence of acetic acid formed from PAA decomposition [87].

Finally, the appearance of a new peak around 8.1 ppm may be attributed to oxidized species formed during the PAA treatment, likely formic acid [88], [89] or other degradation products [90], consistent with the oxidative delignification conditions employed.

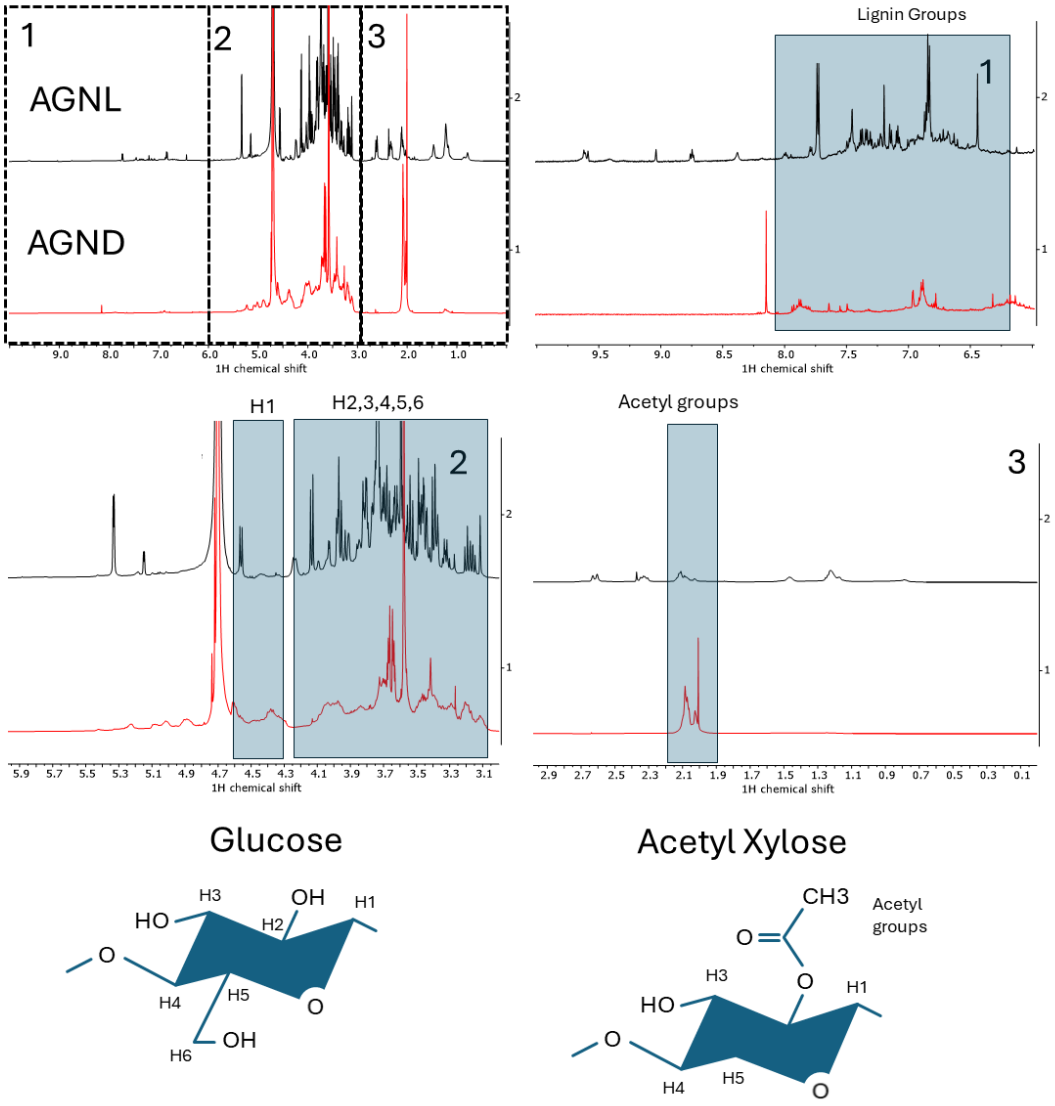


Figure 22: ^{1}H NMR spectra of aqueous extracts acquired in D_2O for lignified (black) and delignified (red) samples.

Upon exposure of the lignified aspen biomass to $NaIO_4$ (AGPL), significant spectral changes were observed within the first 20 minutes (Figure 23): the broad carbohydrate resonances between 3.0 and 5.5 ppm decreased indicating rapid oxidation of vicinal diols in polysaccharides, [38], [40], [91], with the accompanying C-C bond cleavage and ring opening, generating dialdehyde structures and further inducing partial depolymerization [77]. Concurrently, new signals appear at approximately 5.0 ppm, 4.75 ppm, 3.5 ppm, and most prominently at 8.3 ppm. The increase of signals around 5.0 ppm likely reflects hemiacetal structures formed from oxidized carbohydrate fragments, while enhancement of signals near 3.5 ppm is consistent with protons adjacent to newly formed carbonyl groups in open-chain or partially oxidized sugar units [40]. The strong emergence of a signal at approximately 8.3 ppm suggests the formation of oxidation products, most plausibly formic acid or formate, arising from secondary oxidative cleavage reactions [89], [92]. After 60 minutes of the reaction, the spectrum simplifies considerably, with only a few residual signals remaining between 3.5 and 3.7 ppm, a signal in the 4.75–4.85 ppm region (indicative of hydrated aldehyde structures)[59], and a very sharp and intense peak at 8.37 ppm. The disappearance of most carbohydrate resonances indicates extensive degradation of polysaccharide structures, leading either to highly oxidized species or to degradation products that dominate the spectrum. The persistence of signals at 3.5–3.7 ppm and 4.75–4.85 ppm suggests the presence of remaining hydrated aldehyde functionalities and oxidized carbohydrate fragments, [40], [59]. The sharp peak at 8.37 ppm, which becomes dominant at longer reaction time, strongly indicates accumulation of formic acid or formate as a major final oxidation product [92]. Altogether, the spectral evolution from 20 to 60 minutes demonstrates progression from initial dialdehyde formation to more extensive oxidative degradation, overoxidation of carbohydrate structures and accumulation of degradation carboxylic acid products in the aqueous phase.

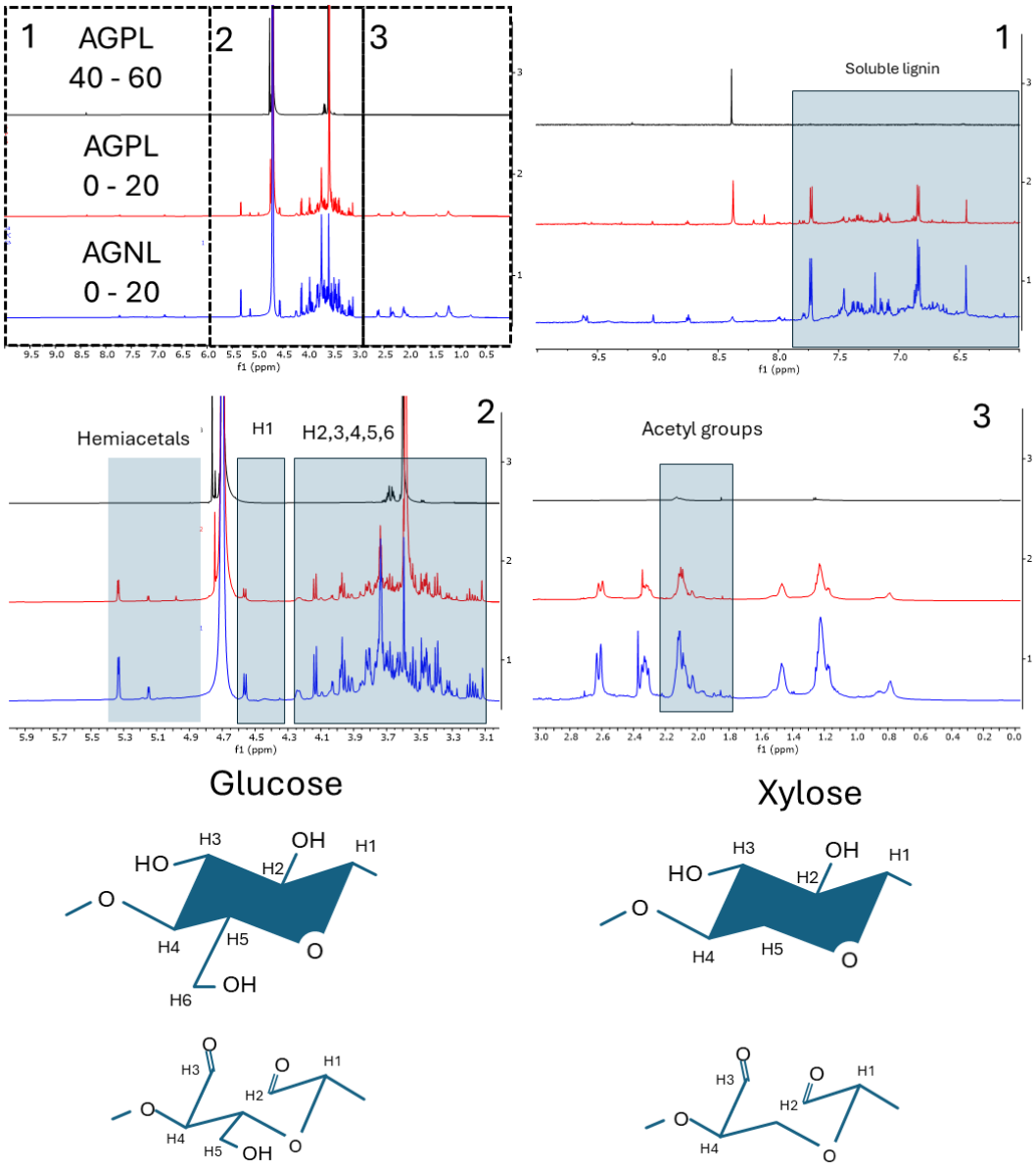


Figure 23: ^{1}H NMR spectra of the obtained extracts acquired in D_2O for lignified samples treated with periodate for 0 – 20 (red), 40 – 60 min (black) and extracted with water for 0-20 min (blue, reference).

Similar spectral behavior was observed also in the HSQC spectra: intense carbohydrate correlations observed in the aqueous extract from the lignified aspen biomass (anomeric cross-peaks at 4.4/100–105 ppm, ring protons at 3.2–4.0/70–80 ppm and methylene protons at 3.6–3.9/60–65 ppm [93], [94]) were reduced upon sodium periodate oxidation already within 20 minutes and accompanied by the emergence of new cross-peaks diagnostic of hydrated aldehydes (4.7–4.85 ppm and 90–95 ppm) [95] and those attributed to degradation products, such as hydroxy acids (2.65 ppm/40–45 ppm); after 40

minutes of reaction time, the extensive oxidative transformation led to a near-total disappearance of the original carbohydrate correlations, leaving the spectrum dominated by signals from oxidized structures and degradation products [95].

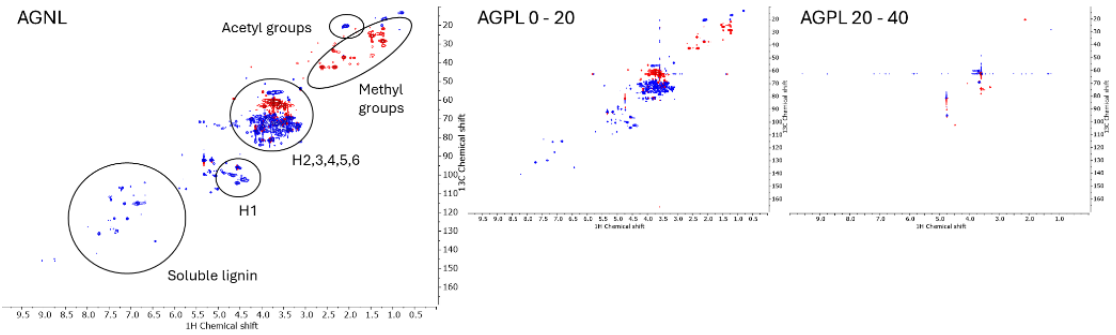


Figure 24: $^{1}H,^{13}C$-HSQCNMR spectra of the obtained extracts acquired in D_2O for lignified samples. AGNL 0 – 20 min (reference) and AGPL 0 -20 and 20 – 40 mins

Upon sodium periodate oxidation of delignified aspen biomass, the ^{1}H NMR spectrum shows significant changes compared to the lignified material (Figure 25). Within the first 20 minutes, the delignified sample exhibits enhanced accessibility of cellulose and hemicellulose, resulting in a more pronounced formation of hydrated aldehyde (gem-diol) species compared to the lignified sample, observed as multiple peaks between 4.7 and 5.0 ppm arising from newly exposed vicinal diols. The peaks around 2.0–2.65 ppm, associated with acetyl groups, decrease due to oxidation. After 60 minutes, most carbohydrate resonances vanish, leaving residual signals between 3.2 and 3.8 ppm attributed to oxidized carbohydrate fragments, along with a small peak at 2.65 ppm. These spectral features indicate that delignification increases the accessibility of polysaccharides to oxidation, generating a broader range of oxidized carbohydrate species and water-soluble byproducts.

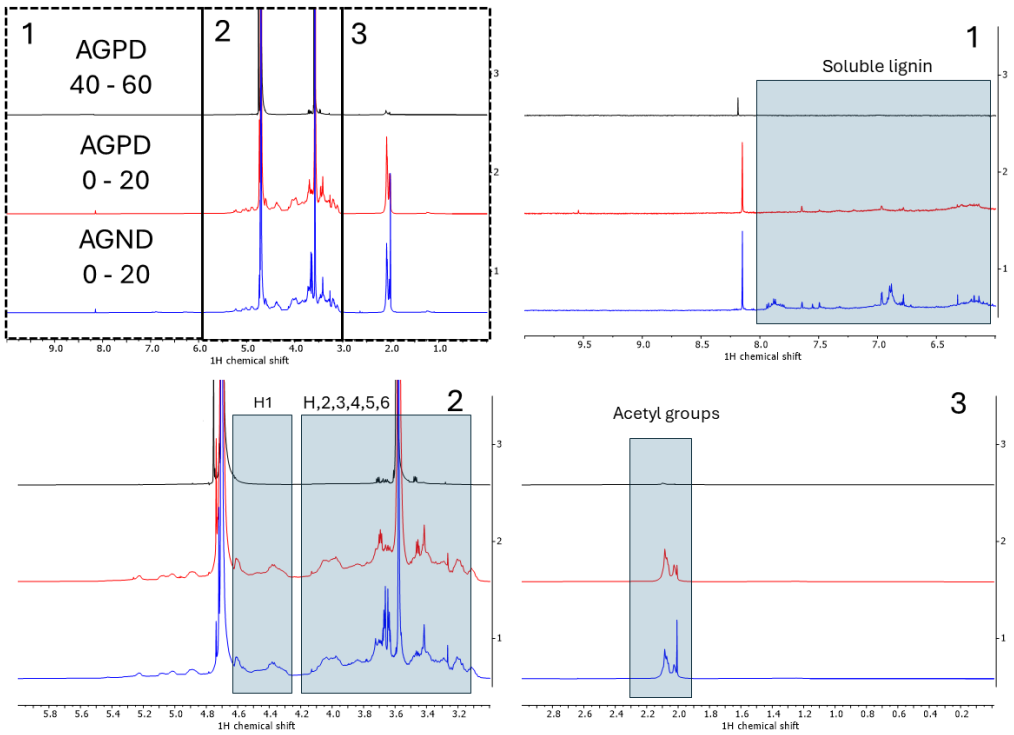


Figure 25: ^{1}H NMR spectra of the obtained extracts acquired in D_2O for delignified samples treated with water from 0-20 min (blue) and for oxidized samples from 0 – 20 (red) and 40 – 60 min (black).

This is also in line with the spectral behavior observed in the HSQC spectra of delignified samples(Figure 26), showing predominantly carbohydrate correlations between 3-5/60–100 ppm and the H-C correlation in the region 4.5-5.5/60-80 (related to hemiacetal groups [40]) when compared to lignified samples. Aromatic lignin correlations and methyl groups are more absent due to the delignification. Acetyl groups are more pronounced near 2.0–2.2 ppm, which may result from the presence of acetic acid formed from the PAA decomposition [87]. Upon the periodate treatment, these signals diminish significantly.

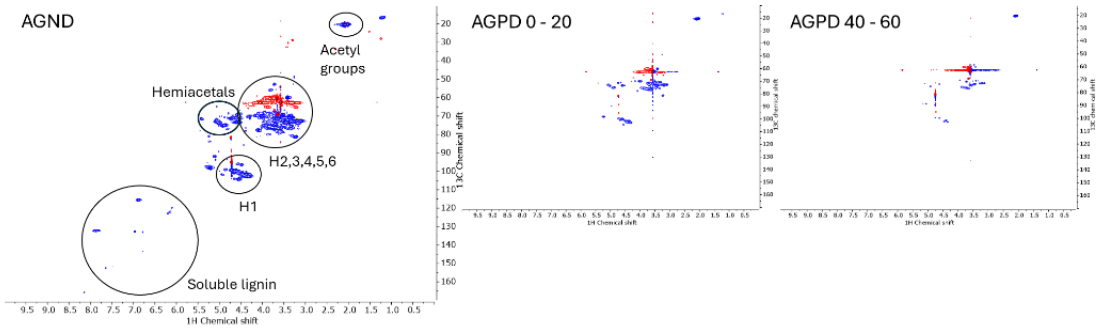


Figure 26: $^{1}H,^{13}C$-HSQCNMR spectra of the obtained extracts acquired in D_2O for delignified samples. AGND 0 – 20 min (reference) and AGPD 0 -20 and 20 – 40 mins.

5. Conclusions

This work investigated sodium periodate oxidation as a strategy to facilitate the extraction of hemicellulose-derived structures from lignocellulosic biomass and to improve the understanding of structural factors governing this process.

The results demonstrate that periodate oxidation can be applied directly to untreated biomass, significantly enhancing the solubilization of carbohydrate-rich fractions without the need for extensive pretreatment. The oxidation process proceeds rapidly, with fast oxidant consumption and early formation of aldehyde functionalities within the carbohydrate structures. These aldehydes subsequently readily undergo secondary reactions such as hydration and hemiacetal crosslinking, while oxidative cleavage leads to depolymerization and decreases the molar mass of the solubilized structures. In addition to the soluble fractions, the solid residues were also chemically modified, as indicated by increased aldehyde content and pseudo-lignin formation during Klason lignin analysis.

Increasing oxidant loading improved extraction efficiency but also promoted crosslinking, degradation, and overoxidation. These findings highlight the importance of optimizing oxidation conditions to balance extraction yield and chemical functionality.

The influence of biomass structure was further evaluated by modifying cell wall accessibility using genetically modified aspen containing callose and selective delignification with peracetic acid. While neither lignin removal nor the introduction of callose spacers significantly affected overall extraction yields, lignin strongly influenced the composition of the extracted fractions. Extracts from lignified samples contained mainly glucose-based residues together with oxidized structures, whereas delignified samples produced extracts enriched in xylose-based carbohydrates.

Despite improved accessibility, due to delignification, oxidation efficiency remained inherently limited. Aldehyde formation occurred mainly at early stages of the reaction, while prolonged oxidation led to further depolymerization. The extracts displayed similar molar mass distributions regardless of biomass modification, indicating that the extension of oxidation plays a dominant role in determining the final product characteristics.

Overall, the results show that periodate oxidation can enable extraction and modification of hemicellulose-derived structures from wood biomass. However, the intrinsically degrading nature of the process largely governs extraction yield and molar mass of the extracts. Specifically, the observed decrease in molar mass alongside the formation of aldehyde functionalities highlights the trade-off between functionalization and polymer degradation.

These results contribute to a better understanding of the structure–reactivity relationships involved in oxidation-mediated biomass processing and support the development of improved strategies for hemicellulose valorization in future biorefineries.

6. Acknowledgments

This research was funded by the Wallenberg Wood Science Center (WWSC).

I would also like to sincerely thank the following people for their support, which made the completion of this thesis possible:

- Professor Merima Hasani, for giving me the opportunity to explore the field of lignocellulose, and for her continuous support, patience, guidance, and motivation throughout this journey.
- Michael Andersson-Sarning and Patrik Skansen, for their exceptional technical expertise and invaluable contributions in the lab. I also greatly appreciated the meaningful conversations during lunch breaks.
- Johanna Spång, for her administrative support related to this thesis, and for keeping the spirit of the division high through organizing holiday events and fikas.
- My best friend Emanuella, whom I had the pleasure of meeting during my PhD. She may not have made my work more efficient, but she certainly made the process much more enjoyable.
- All my colleagues on the third floor, for fostering a welcoming, collaborative, and positive working environment.

I would also like to thank WWSC not only for providing financial support but also for creating a strong network for sharing ideas and advancing research. In addition, I am grateful to Chalmers University of Technology for offering an excellent structure and environment that enabled me to perform my work at my best.

Last but not least, I would like to express my deepest gratitude to my family for their unconditional love and support throughout my life. Also, I'm especially grateful to my girlfriend, Deborah, for her love and for always making me smile.

7. References

[1] F. G. Calvo-Flores and F. J. Martin-Martinez, “Biorefineries: Achievements and challenges for a bio-based economy,” *Front. Chem.*, vol. 10, pp. 1–23, Nov. 2022, doi: 10.3389/fchem.2022.973417.

[2] F. Mathura, A. Gabriela, A. Sosa, and L. M. Orejuela-escobar, “Hemicelluloses from bioresidues and their applications in the food industry – towards an advanced bioeconomy and a sustainable global food system,” *Sustain. Food Technol.*, vol. 2, pp. 628-646, 2024, doi: 10.1039/d4fb00035h.

[3] J. Wojtasz-Mucha, M. Hasani, and H. Theliander, “Hydrothermal pretreatment of wood by mild steam explosion and hot water extraction,” *Bioresour. Technol.*, vol. 241, pp. 120–126, Oct. 2017, doi: 10.1016/j.biortech.2017.05.061.

[4] J. A. Okolie, S. Nanda, A. K. Dalai, and J. A. Kozinski, “Chemistry and Specialty Industrial Applications of Lignocellulosic Biomass,” *Waste Biomass Valorization*, vol. 12, no. 5, pp. 2145–2169, 2021, doi: 10.1007/s12649-020-01123-0.

[5] D. Pérez-Almada, Á. Galán-Martín, M. del M. Contreras, and E. Castro, “Integrated techno-economic and environmental assessment of biorefineries: review and future research directions,” *Sustainable Energy Fuels*, vol. 7, pp. 3316-3335, 2023, doi: 10.1039/d3se00405h.

[6] A. O. Ojo, “An Overview of Lignocellulose and Its Biotechnological Importance in High-Value Product Production,” *Fermentation*, vol. 9, no. 11, p. 990, 2023, doi: 10.3390/fermentation9110990.

[7] M. Hu, J. Chen, Y. Yu, and Y. Liu, “Peroxyacetic Acid Pretreatment: A Potentially Promising Strategy towards Lignocellulose Biorefinery,” *Molecules*, vol. 27, no. 19, p. 6359, Oct. 2022, doi: 10.3390/molecules27196359.

[8] M. M. Abu-Omar, K. Barta, G. T. Beckham, J. S. Luterbacher, J. Ralph, R. Rinaldi, J. S. M. Vandezande, and T. J. Wood, “Guidelines for performing lignin-first biorefining,” *Energy Environ. Sci.*, vol. 14, no. 1, pp. 262-292, 2021, doi: 10.1039/d0ee02870c.

[9] B. Segers, S. Sels, S. Van den Bosch, J. G. Rosenboom, and B. F. Sels, “Lignocellulosic biomass valorisation: a review of feedstocks, processes and potential value chains and their implications for the decision-making process,” *RSC Sustainability*, vol. 2, pp. 3173-3199, 2024, doi: 10.1039/d4su00342j.

[10] C. Chen, Y. Kuang, S. Zhu, I. Burgert, T. Keplinger, A. Gong, T. Li, L. Berglund, S. J. Eichhorn, and L. Hu, “Structure–property–function relationships of natural and engineered wood,” *Nat. Rev. Mater.*, vol. 5, no. 9, pp. 642–666, Sep. 2020, doi: 10.1038/s41578-020-0195-z.

[11] G. Henriksson and H. Lennholm, *Wood Chemistry and Wood Biotechnology*, vol. 1. Berlin: Walter de Gruyter, 2009, doi: 10.1515/9783110213409.

[12] A. A. Chaudhari, S. S. Moholkar, S. R. Meshram, and V. B. Patravale, “Modifying lignin composition and xylan O-acetylation induces changes in cell wall composition, extractability, and digestibility,” *Biotechnol. Biofuels Bioprod.*, vol. 17, no. 1, p. 102, 2024, doi: 10.1186/s13068-024-02513-5.

[13] F. H. Isikgor and C. R. Becer, “Lignocellulosic biomass: a sustainable platform for the production of bio-based chemicals and polymers,” *Polym. Chem.*, vol. 6, no. 25, pp. 4497–4559, Jul. 2015, doi: 10.1039/c5py00263j.

[14] P. Sivan, A. Martinsson, M. Hasani, and H. Theliander, “Sequential extraction of hemicelluloses by subcritical water improves saccharification of hybrid aspen wood grown in greenhouse and field conditions,” *Green Chem.*, vol. 25, no. 14, pp. 5634–5646, Jun. 2023, doi: 10.1039/d3gc01020a.

[15] T.-Y. Hsieh, “Structure/properties relationships of time-dependent behavior of wood—from understanding mechanisms to determining predictive indicators,” Ph.D. dissertation, Univ. Montpellier, Montpellier, France, 2022.

[16] J. Rao, Z. Lv, G. Chen, and F. Peng, “Hemicellulose: Structure, chemical modification, and application,” *Prog. Polym. Sci.*, vol. 140, p. 101675, 2023, doi: 10.1016/j.progpolymsci.2023.101675.

[17] J. Berglund, S. J. Merali, J. S. M. Vandezande, G. Henriksson, M. E. Lindström, and J. Wohlert, “Wood hemicelluloses exert distinct biomechanical contributions to cellulose fibrillar networks,” *Nat. Commun.*, vol. 11, no. 1, p. 4692, Dec. 2020, doi: 10.1038/s41467-020-18390-z.

[18] A. Teleman, M. Tenkanen, A. Jacobs, and O. Dahlman, “Characterization of O-acetyl-(4-O-methylglucurono)xylan isolated from birch and beech,” *Carbohydr. Res.*, vol. 337, no. 4, pp. 373–377, 2002, doi: 10.1016/S0008-6215(01)00327-5.

[19] S. Willför, R. Sjöholm, C. Laine, M. Roslund, J. Hemming, and B. Holmbom, “Characterisation of water-soluble galactoglucomannans from Norway spruce wood and thermomechanical pulp,” *Carbohydr. Polym.*, vol. 52, no. 2, pp. 175–187, May 2003, doi: 10.1016/S0144-8617(02)00288-6.

[20] Y. Yoshimi, T. Tryfona, and P. Dupree, “Structure, Modification Pattern, and Conformation of Hemicellulose in Plant Biomass,” *J. Appl. Glycosci.*, vol. 71, no. 1, pp. 1-11, 2024, doi: 10.5458/jag.7201301.

[21] F. Abik, G. Tedeschi, A. S. Moretti, and M. G. Tuohy, “Potential of Wood Hemicelluloses and Their Derivates as Food Ingredients,” *J. Agric. Food Chem.*, vol. 71, no. 14, pp. 5414–5431, 2023, doi: 10.1021/acs.jafc.2c06449.

[22] D. S. Naidu, S. P. Hlangothi, and M. J. John, “Bio-based products from xylan: A review,” *Carbohydr. Polym.*, vol. 179, pp. 28–41, 2018, doi: 10.1016/j.carbpol.2017.09.064.

[23] J. Tuteja and A. Sand, “Introductory Chapter: Introduction to Structure Properties and Application of Lignin,” in *Lignin - Chemistry, Structure, and Application*, Rijeka: IntechOpen, 2023, doi: 10.5772/intechopen.110024.

[24] D. Tarasov, M. Leitch, and P. Fatehi, “Lignin-carbohydrate complexes: Properties, applications, analyses, and methods of extraction: A review,” *Biotechnol. Biofuels*, vol. 11, no. 1, p. 269, Sep. 2018, doi: 10.1186/s13068-018-1262-1.

[25] N. Giummarella, L. Zhang, G. Henriksson, and M. Lawoko, “Structural features of mildly fractionated lignin carbohydrate complexes (LCC) from spruce,” *RSC Adv.*, vol. 6, no. 48, pp. 42120–42131, 2016, doi: 10.1039/c6ra02399a.

[26] E. Heinonen, G. Henriksson, M. E. Lindström, F. Vilaplana, and J. Wohlert, “Xylan adsorption on cellulose: Preferred alignment and local surface immobilizing effect,” *Carbohydr. Polym.*, vol. 285, p. 119221, Jun. 2022, doi: 10.1016/j.carbpol.2022.119221.

[27] N. Zhang, S. Li, L. Xiong, Y. Hong, and Y. Chen, “Cellulose-hemicellulose interaction in wood secondary cell-wall,” *Model. Simul. Mater. Sci. Eng.*, vol. 23, no. 8, p. 085010, Oct. 2015, doi: 10.1088/0965-0393/23/8/085010.

[28] D. Mboowa, “A review of the traditional pulping methods and the recent improvements in the pulping processes,” *Biomass Convers. Biorefin.*, vol. 14, no. 1, pp. 1–15, 2024, doi: 10.1007/s13399-020-01243-6.

[29] W. Farhat, “Investigation of hemicellulose biomaterial approaches: the extraction and modification of hemicellulose and its use in value-added applications,” Ph.D. dissertation, Univ. Grenoble Alpes, France, 2019. [Online]. Available: HAL Id: tel-02305657.

[30] Y. Lu, Q. He, G. Fan, Q. Cheng, and G. Song, “Extraction and modification of hemicellulose from lignocellulosic biomass: A review,” *Green Process. Synth.*, vol. 10, no. 1, pp. 779–804, Nov. 2021, doi: 10.1515/gps-2021-0065.

[31] T. V. Vuong, L. G. Thygesen, C. Felby, and S. Brumer, “Enzymatic Routes to Designer Hemicelluloses for Use in Biobased Materials,” *JACS Au*, vol. 4, no. 11, pp. 4100-4115, 2024, doi: 10.1021/jacsau.4c00469.

[32] A. F. Ainani, J. T. Rubiyanto, M. N. Ardian, W. N. Habiba, A. Syarifuddin, and A. Dirpan, “Hemicellulose-Based Hydrogel Composite: Enhanced Properties and Diverse Applications,” *Carbohydr. Polym. Technol. Appl.*, p. 100558, 2024, doi: 10.1016/j.carpta.2024.100558.

[33] T. Nypelö, B. Berke, S. Spirk, and J. A. Sirviö, “Review: Periodate oxidation of wood polysaccharides—Modulation of hierarchies,” *Carbohydr. Polym.*, vol. 252, p. 117105, Jan. 2021, doi: 10.1016/j.carbpol.2020.117105.

[34] A. Martinsson, M. Hasani, and H. Theliander, “Physical properties of kraft pulp oxidized by hydrogen peroxide under mildly acidic conditions,” *Nord.*

Pulp Paper Res. J., vol. 37, no. 2, pp. 330–337, 2022, doi: 10.1515/npprj-2022-0020.

[35] Y. Okita, T. Saito, and A. Isogai, “Entire surface oxidation of various cellulose microfibrils by TEMPO-mediated oxidation,” *Biomacromolecules*, vol. 11, no. 6, pp. 1696–1700, Jul. 2010, doi: 10.1021/bm100214b.

[36] M. Börjesson, A. Larsson, G. Westman, and A. Ström, “Periodate oxidation of xylan-based hemicelluloses and its effect on their thermal properties,” *Carbohydr. Polym.*, vol. 202, pp. 280–287, 2018, doi: 10.1016/j.carbpol.2018.08.110.

[37] M. Chemin, S. P. Chollet, S. Guillot, J. Le Coz, and V. Villari, “Periodate oxidation of 4-O-methylglucuronoxylans: Influence of the reaction conditions,” *Carbohydr. Polym.*, vol. 142, pp. 45–50, 2016, doi: 10.1016/j.carbpol.2016.01.025.

[38] C. Palasingh, P. S. S. Prasad, S. R. Meshram, and V. B. Patravale, “Modification of xylan via an oxidation–reduction reaction,” *Carbohydr. Polym.*, vol. 292, p. 119660, Sep. 2022, doi: 10.1016/j.carbpol.2022.119660.

[39] C. O. Pandeirada, S. Boulos, and L. Nyström, “Oxidized polysaccharides: A review on structural insights using MS-based approaches,” *Carbohydr. Polym.*, vol. 350, p. 123946, 2025, doi: 10.1016/j.carbpol.2025.123946.

[40] H. Amer, K. N. S. Schmidt, K. H. S. Sjöberg, and T. Rosenau, “Synthesis and Characterization of Periodate-Oxidized Polysaccharides: Dialdehyde Xylan (DAX),” *Biomacromolecules*, vol. 17, no. 9, pp. 2972–2980, 2016, doi: 10.1021/acs.biomac.6b00777.

[41] M. Bourdon, D. Pirone, L. M. G. Thygesen, and S. Brumer, “Ectopic callose deposition into woody biomass modulates the nano-architecture of macrofibrils,” *Nat. Plants*, vol. 9, no. 9, pp. 1530–1546, Sep. 2023, doi: 10.1038/s41477-023-01459-0.

[42] L. Xu and U. Tschirner, “Peracetic acid pretreatment of alfalfa stem and aspen biomass,” *Bioresources*, vol. 7, no. 1, pp. 203–216, Nov. 2011, doi: 10.15376/biores.7.1.203-216.

[43] R. Ma, W. Hao, X. Ma, Y. Tian, and J. Li, “Role of peracetic acid on the disruption of lignin packing structure and its consequence on lignin depolymerisation,” *Green Chem.*, vol. 23, no. 21, pp. 8468–8479, Nov. 2021, doi: 10.1039/d1gc02300d.

[44] S. Y. Park, H. J. Bae, K. S. Han, and J. S. Kim, “Peracetic acid-induced kraft lignin solubilization and its characterization for selective production of macromolecular biopolymers,” *Int. J. Biol. Macromol.*, vol. 161, pp. 1240–1246, Oct. 2020, doi: 10.1016/j.ijbiomac.2020.06.041.

[45] R. Kumar, F. Hu, C. A. Hubbell, A. J. Ragauskas, and C. E. Wyman, “Comparison of laboratory delignification methods, their selectivity, and impacts on physiochemical characteristics of cellulosic biomass,” *Bioresour. Technol.*, vol. 130, pp. 372–381, 2013, doi: 10.1016/j.biortech.2012.12.028.

[46] H. Zhao and N. D. Heindel, “Determination of degree of substitution of formyl groups in polyaldehyde dextran by the hydroxylamine hydrochloride method,” *Pharm. Res.*, vol. 8, no. 3, pp. 400-402, 1991, doi: 10.1023/a:1015866104055.

[47] K. Babor, V. Kaláč, and K. Tihlárik, “Periodate oxidation of saccharides. III. Comparison of the methods for determining the consumption of sodium periodate and the amount of formic acid formed,” *Chem. Pap.*, vol. 27, no. 5, pp. 676–680, 1973.

[48] L. C. A. Barbosa, C. R. A. Maltha, A. J. Demuner, C. M. Cazal, E. L. Reis, and J. L. Colodette, “A rapid method for quantification of carboxyl groups in cellulose pulp,” *O Papel*, vol. 74, no. 1, pp. 45-50, 2013. doi: 10.4334/PULP.2013.001-1043.

[49] A. Sluiter, B. Hames, R. Ruiz, C. Scarlata, J. Sluiter, D. Templeton, and D. Crocker, “Determination of structural carbohydrates and lignin in Biomass,” *NREL Tech. Rep.*, NREL/TP-510-42618, 2008.

[50] S. Zhu, T. Song, T. Han, H. Qi, P. Liu, and T. Rosenau, “The bifunctionality of glucurono-dialdehyde xylan (GlcU-DAX) in the preparation of silver nanoparticles with optimized size, size distribution and dispersibility: a mechanistic study,” *Cellulose*, vol. 32, no. 9, pp. 5301–5320, Jun. 2025, doi: 10.1007/s10570-025-06459-1.

[51] C. G. Gomez, M. Rinaudo, and M. A. Villar, “Oxidation of sodium alginate and characterization of the oxidized derivatives,” *Carbohydr. Polym.*, vol. 67, no. 3, pp. 296–304, 2007, doi: 10.1016/j.carbpol.2006.05.025.

[52] Y. Nishiyama, U. J. Kim, D. Y. Kim, K. S. Katsumata, R. P. May, and P. Langan, “Periodic disorder along ramie cellulose microfibrils,” *Biomacromolecules*, vol. 4, no. 4, pp. 1013–1017, Jul. 2003, doi: 10.1021/bm025772x.

[53] C. O. Pandeirada, M. Achterweust, H. G. Janssen, Y. Westphal, and H. A. Schols, “Periodate oxidation of plant polysaccharides provides polysaccharide-specific oligosaccharides,” *Carbohydr. Polym.*, vol. 291, p. 119540, Sep. 2022, doi: 10.1016/j.carbpol.2022.119540.

[54] J. Janson, “Analytik der polysaccharide in Holz und Zellstoff,” *Faserforschung und Textiltechnik*, vol. 25, no. 9, pp. 375–382, 1974.

[55] R. M. Rowell, *Handbook of Wood Chemistry and Wood Composites*. 1st ed. Boca Raton: CRC Press, 2005, doi: 10.1201/9780203492437.

[56] C. C. Piras, S. Fernández-Prieto, and W. M. De Borggraeve, “Ball milling: A green technology for the preparation and functionalisation of nanocellulose derivatives,” *Nanoscale Adv.*, vol. 1, no. 3, pp. 937–947, 2019, doi: 10.1039/c8na00238j.

[57] L. Fliri, J. Simon, I. Sulaeva, T. Rosenau, A. Potthast, and M. Hummel, “Indirect determination of partial depolymerization reactions in dialdehyde celluloses (DAC) by gel permeation chromatography of their oxime

derivatives," *Cellulose*, vol. 30, no. 14, pp. 8677–8690, Sep. 2023, doi: 10.1007/s10570-023-05412-4.

[58] A. Chetouani, S. El-Ghrablwy, M. Meddich, M. El-Amraoui, and S. El-Habbak, "Physicochemical properties and biological activities of novel blend films using oxidized pectin/chitosan," *Int. J. Biol. Macromol.*, vol. 97, pp. 348–356, Apr. 2017, doi: 10.1016/j.ijbiomac.2017.01.018.

[59] J. Sasaki and P. Kosma, "β-Elimination as major side reaction in periodate-oxidation of cellulosic model mono- and disaccharides," *Monatsh. Chem.*, vol. 156, no. 1, pp. 3–13, Jan. 2025, doi: 10.1007/s00706-023-03146-4.

[60] D. Paiva, C. Gonçalves, I. Vale, M. M. S. M. Bastos, and F. D. Magalhães, "Oxidized Xanthan Gum and Chitosan as Natural Adhesives for Cork," *Polymers*, vol. 8, no. 7, p. 259, Jul. 2016, doi: 10.3390/polym8070259.

[61] J. Simon, L. Fliri, I. Sulaeva, A. Potthast, and T. Rosenau, "Insights into the borohydride reduction of dialdehyde cellulose: the dilemma of competing reduction and β-elimination reactions," *Cellulose*, vol. 30, no. 13, pp. 8205–8220, Sep. 2023, doi: 10.1007/s10570-023-05350-1.

[62] P. Tangthuam, J. Pimoei, A. A. Mohamad, F. Mahlendorf, A. Somwangthanaroj, and S. Kheawhom, "Carboxymethyl cellulose-based polyelectrolyte as cationic exchange membrane for zinc-iodine batteries," *Heliyon*, vol. 6, no. 10, p. e05391, Oct. 2020, doi: 10.1016/j.heliyon.2020.e05391.

[63] H. Ge, L. Zhang, M. Xu, J. Cao, and C. Kang, "Preparation of Dialdehyde Cellulose and Its Antibacterial Activity," in *International Conference on Applied Biotechnology*, Singapore: Springer, 2016, pp. 545–553.

[64] U. J. Kim, S. Kuga, M. Wada, T. Okano, and T. Kondo, "Periodate oxidation of crystalline cellulose," *Biomacromolecules*, vol. 1, no. 3, pp. 488–492, 2000, doi: 10.1021/bm0000337.

[65] A. Teleman, M. Nordström, M. Tenkanen, A. Jacobs, and O. Dahlman, "Isolation and characterization of O-acetylated glucomannans from aspen and birch wood," *Carbohydr. Res.*, vol. 338, no. 6, pp. 525–534, Mar. 2003, doi: 10.1016/S0008-6215(02)00491-3.

[66] P. Sannigrahi, D. H. Kim, S. Jung, and A. Ragauskas, "Pseudo-lignin and pretreatment chemistry," *Energy Environ. Sci.*, vol. 4, no. 4, pp. 1306–1310, Mar. 2011, doi: 10.1039/c0ee00378f.

[67] N. Chen, K. Jiang, M. Zhao, C. Zhang, Y. Jin, and W. Wu, "Pretreatment process of lignocellulosic biomass: A review of pseudo-lignin formation," *Biomass Bioenergy*, vol. 188, p. 107339, Sep. 2024, doi: 10.1016/j.biombioe.2024.107339.

[68] J. Lundqvist, A. Teleman, L. Junel, G. Zacchi, O. Dahlman, and P. Stalbrand, "Isolation and characterization of galactoglucomannan from

spruce (Picea abies)," *Carbohydr. Polym.*, vol. 48, no. 1, pp. 29–39, Apr. 2002, doi: 10.1016/S0144-8617(01)00210-7.

[69] C. Kundu, S. P. Samudrala, M. A. Kibria, and S. Bhattacharya, "One-step peracetic acid pretreatment of hardwood and softwood biomass for platform chemicals production," *Sci. Rep.*, vol. 11, no. 1, p. 11090, Dec. 2021, doi: 10.1038/s41598-021-90667-9.

[70] M. Balakshin, E. Capanema, H. Gracz, H. M. Chang, and H. Jameel, "Quantification of lignin-carbohydrate linkages with high-resolution NMR spectroscopy," *Planta*, vol. 233, no. 6, pp. 1097–1110, Jun. 2011, doi: 10.1007/s00425-011-1359-2.

[71] M. Lawoko, G. Henriksson, and G. Gellerstedt, "Structural Differences between the Lignin-Carbohydrate Complexes Present in Wood and in Chemical Pulps," *Biomacromolecules*, vol. 6, no. 6, pp. 3467-3473, 2005, doi: 10.1021/bm058014q.

[72] T. Watanabe, J. Ohnishi, Y. Yamasaki, S. Kaizu, and T. Koshijima, "Binding-site analysis of the ether linkages between lignin and hemicelluloses in lignin-carbohydrate complexes by DDQ-oxidation," *Agric. Biol. Chem.*, vol. 53, no. 8, pp. 2233–2252, 1989, doi: 10.1080/00021369.1989.10869603.

[73] W. Geng, R. A. Venditti, J. J. Pawlak, and H. Chang, "Effect of delignification on hemicellulose extraction from switchgrass, poplar, and pine and its effect on enzymatic convertibility of cellulose-rich residues," *Bioresources*, vol. 13, no. 3, pp. 4946–4963, May 2018, doi: 10.15376/biores.13.3.4946-4963.

[74] H. R. Lee, R. J. Kazlauskas, and T. H. Park, "One-step pretreatment of yellow poplar biomass using peracetic acid to enhance enzymatic digestibility," *Sci. Rep.*, vol. 7, no. 1, p. 12111, Dec. 2017, doi: 10.1038/s41598-017-12542-w.

[75] P. M. A. Pawar, K. Ratke, B. K. Balasubramanian, S. J. Merali, S. B. Brumer, and E. J. Mellerowicz, "In muro deacetylation of xylan affects lignin properties and improves saccharification of aspen wood," *Biotechnol. Biofuels*, vol. 10, no. 1, p. 98, Apr. 2017, doi: 10.1186/s13068-017-0782-4.

[76] Z. Zhai and K. J. Edgar, "Polysaccharide Aldehydes and Ketones: Synthesis and Reactivity," *Biomacromolecules*, vol. 25, no. 5, pp. 2655–2690, 2024, doi: 10.1021/acs.biomac.4c00020.

[77] K. A. Kristiansen, A. Potthast, and B. E. Christensen, "Periodate oxidation of polysaccharides for modification of chemical and physical properties," *Carbohydr. Res.*, vol. 345, no. 10, pp. 1264–1271, Jul. 2010, doi: 10.1016/j.carres.2010.02.011.

[78] M. S. Tunc, M. Lawoko, and A. van Heiningen, "Understanding the limitations of removal of hemicelluloses during autohydrolysis of a mixture of Southern hardwoods," *Bioresources*, vol. 5, no. 1, pp. 356–371, Jan. 2010, doi: 10.15376/biores.5.1.356-371.

[79] A. Martínez-Abad, N. Giummarella, M. Lawoko, and F. Vilaplana, “Differences in extractability under subcritical water reveal interconnected hemicellulose and lignin recalcitrance in birch hardwoods,” *Green Chem.*, vol. 20, no. 11, pp. 2534–2546, 2018, doi: 10.1039/c8gc00385h.

[80] L. K. Azambuja and M. Hasani, “Sodium periodate mediated oxidative extraction of polysaccharide-derived structures from wood biomass: Influence of reaction time and oxidation conditions in birch and spruce,” *Bioresources*, vol. 21, no. 2, pp. 2960–2979, 2026, doi: 10.15376/biores.21.2.2960-2979.

[81] Q. Luo, X. F. Cao, R. C. Sun, and F. Peng, “Alkali extraction and physicochemical characterization of hemicelluloses from young bamboo (Phyllostachys pubescens Mazel),” *Bioresources*, vol. 7, no. 4, pp. 5817–5828, Oct. 2012, doi: 10.15376/biores.7.4.5817-5828.

[82] J. Duus, C. H. Gotfredsen, and K. Bock, “Carbohydrate structural determination by NMR spectroscopy: modern methods and limitations,” *Chem. Rev.*, vol. 100, no. 12, pp. 4589–4614, Dec. 2000, doi: 10.1021/cr990302n.

[83] J. Dou, M. Kögler, K. K. Kesari, L. Pitkänen, and T. Vuorinen, “Seasonal dynamics in structural characteristics within bark stems of cultivated willow (Salix sp.) by NMR and time-gated Raman spectroscopy,” *Green Chem.*, vol. 25, no. 5, pp. 1908–1919, Jan. 2023, doi: 10.1039/d2gc04476e.

[84] T. Sathasivam, N. S. J. K. G. L. Kumar, S. S. Moholkar, and V. B. Patravale, “Facile Fabrication of Lignin-Cellulose Green Nanogels,” *Chem. Asian J.*, vol. 17, no. 21, p. e202200671, Nov. 2022, doi: 10.1002/asia.202200671.

[85] X. Du, J. Gellerstedt, J. Li, and G. Gellerstedt, “Understanding pulp delignification by laccase-mediator systems through isolation and characterization of lignin-carbohydrate complexes,” *Biomacromolecules*, vol. 14, no. 9, pp. 3073–3080, Sep. 2013, doi: 10.1021/bm4006936.

[86] W. Wang, X. Chen, R. Katahira, and M. Tucker, “Characterization and deconstruction of oligosaccharides in black liquor from deacetylation process of corn stover,” *Front. Energy Res.*, vol. 7, p. 54, Jun. 2019, doi: 10.3389/fenrg.2019.00054.

[87] J. Zhuo, J. Bobokalonov, S. Usmanova, and Z. Xiang, “Effects of peracetic acid delignification on hemicellulose extraction by dimethyl sulfoxide,” *Ind. Crops Prod.*, vol. 222, p. 119731, Dec. 2024, doi: 10.1016/j.indcrop.2024.119731.

[88] A. Maxut, B. Nozière, B. Fenet, and H. Mechakra, “Formation mechanisms and yields of small imidazoles from reactions of glyoxal with NH4+ in water at neutral pH,” *Phys. Chem. Chem. Phys.*, vol. 17, no. 31, pp. 20416–20424, Aug. 2015, doi: 10.1039/c5cp03113c.

[89] F. Caputo, B. Al-Rudainy, P. Naidjonoka, O. Wallberg, L. Olsson, and V. Novy, “Understanding the impact of steam pretreatment severity on cellulose

ultrastructure, recalcitrance, and hydrolyzability of Norway spruce," *Biomass Convers. Biorefin.*, vol. 14, no. 21, pp. 27211–27223, Nov. 2024, doi: 10.1007/s13399-022-03405-0.

[90] T. J. Smak, P. de Peinder, J. C. Van der Waal, R. Altink, I. Vollmer, and B. M. Weckhuysen, "Oxidative Conversion of Polyethylene Towards Di-Carboxylic Acids: A Multi-Analytical Approach," *ChemSusChem*, vol. 17, no. 7, p. e202301198, Apr. 2024, doi: 10.1002/cssc.202301198.

[91] M. Chemin, S. P. Chollet, V. Villari, S. Guillot, and R. Backov, "Synthesis and characterization of functionalized 4-O-methylglucuronoxylan derivatives," *Holzforschung*, vol. 69, no. 6, pp. 713–720, 2015, doi: 10.1515/hf-2014-0290.

[92] H. S. Siebe, J. Sasaki, J. Simon, T. Rosenau, and K. Barta, "Formation of substituted dioxanes in the oxidation of gum arabic with periodate," *Green Chem.*, vol. 25, no. 10, pp. 4058–4066, Apr. 2023, doi: 10.1039/d2gc04923f.

[93] D. J. Yelle, J. Ralph, and C. R. Frihart, "Characterization of nonderivatized plant cell walls using high-resolution solution-state NMR spectroscopy," *Magn. Reson. Chem.*, vol. 46, no. 6, pp. 508–517, 2008, doi: 10.1002/mrc.2201.

[94] J. Rencoret, A. Gutierrez, L. Nieto, J. Jimenez-Barbero, C. Faulds, and A. T. Martinez, "HSQC-NMR analysis of lignin in woody (Eucalyptus globulus and Picea abies) and non-woody (Agave sisalana) ball-milled plant materials at the gel state," *Holzforschung*, vol. 63, no. 6, pp. 691–698, 2009, doi: 10.1515/HF.2009.070.

[95] T. Koso, S. Korhonen, T. Vuorinen, and J. Helminen, "2D Assignment and quantitative analysis of cellulose and oxidized celluloses using solution-state NMR spectroscopy," *Cellulose*, vol. 27, no. 14, pp. 7929–7953, Sep. 2020, doi: 10.1007/s10570-020-03317-0.